1971

Photoionization of photoexcited cesium

Robert E. Hebner

Department: Physics

Cesium
E. Tolle

PHOTOIONIZATION OF PHOTOEXCITED CESIUM

by

ROBERT E. HEBNER, JR., 1945-

A DISSERTATION

Presented to the Faculty of the Graduate School of the

UNIVERSITY OF MISSOURI-ROLLA

In Partial Fulfillment of the Requirements for the Degree

DOCTOR OF PHILOSOPHY

in

PHYSICS

1971

K. T. Nygaard
Advisor

Norman E. Levine

G. A. Sund

William R. Snow

Richard Anderson

ABSTRACT

A new method for obtaining the cross section for photoionization of photoexcited cesium is presented. The salient feature of this experiment is to use three crossed beams, i.e., two light beams intersecting a beam of cesium atoms. The cross section is determined by counting the ions produced by the two step process:

$$Cs\ (6S) + h\nu_1 \rightarrow Cs\ (6P)$$

$$Cs\ (6P) + h\nu_2 \rightarrow Cs^+ + e^-$$

The relative cross section for the second step has been obtained from threshold (5060 Å) to 2500 Å.

The excitation light source used in obtaining this cross section was a rf resonance lamp, but the possibility of using a GaAs laser as this light source was also investigated. A GaAs laser was thermally tuned to the 6S - 6P transition wavelength in cesium, 8521 Å, and it was found that in this way the hyperfine levels of the ground state of cesium could be selectively depopulated. Although excellent results were obtained in this portion of the study, the low duty cycle of the lasers that we had available made them unsuitable for the photoionization experiment.

PREFACE

To improve the clarity of presentation, the material in this dissertation is divided into three parts. The first section discusses the photoionization of photoexcited cesium. The material in this section has been presented at both the VII International Conference of Physics of Electronic and Atomic Collisions, Amsterdam, 1971, and the 24th Annual Gaseous Electronics Conference, Gainsville, Florida, 1971.

The following two parts, one dealing with optical pumping of cesium vapor and the other discussing thermal tuning of GaAs lasers, were spin-off from the basic study of photoionization. Only because they were spin-off and not because the information contained in these sections is any less significant or original are they included as appendices. Since GaAs lasers were inexpensive and thermally tunable to the resonance transitions of cesium, they appeared to be attractive candidates for sources of excitation light in the photoionization experiment. With this in mind, a study of the technical problems of matching a GaAs laser line to cesium resonance transitions was undertaken. It turned out that the low duty cycle of the lasers made them infeasible for the photoionization experiment, but our studies led to a new optical pumping scheme for cesium masers and a deeper insight into the operation of GaAs lasers. Appendix I, has been published in the Journal of the Optical Society of America 61, 1455 (1971) and Appendix II has been accepted for publication in Physica and is presently in press.

I would also like to acknowledge the cooperation from my advisor, Dr. Kaare J. Nygaard. It was his idea that initiated the work and his

continuing advice and support added immeasurably to its successful completion. Beaufort Lancaster, Daniel Kastelein, Yubong Hahn and Daniel Jones have made innumerable day-to-day contributions to this work. For the financial support that enabled me to carry on this program, I would like to thank the Department of Physics, University of Missouri-Rolla, the Office of Naval Research and the National Science Foundation. The faculty of the Physics Department deserves thanks for helping me to develop the scientific maturity necessary for this work. Finally, I would like to thank my wife, Donna Hebner, whose support made my work possible.

TABLE OF CONTENTS

LIST OF ILLUSTRATIONS

PHOTOIONIZATION OF PHOTOEXCITED CESIUM

A. INTRODUCTION

The photoionization process represents a dramatic example of an interaction between electromagnetic radiation and matter. One prerequisite for the process to occur is that the energy of each quantum of radiation be equal to or larger than the ionization energy of the atomic, ionic, or molecular states being studied. The point is worth emphasizing, since the energy required to photoionize an excited state of a certain species is less than that for ionization if the corresponding groundstate, the difference of course, being equal to the excitation energy. (Exceptions as found in high-density, high-temperature plasmas fall outside the scope of this work.)

A multitude of photoionization mechanisms is found in stellar and terrestrial atmospheres, as well as in a number of man-made laboratory plasmas. In astrophysics, for instance, radiative recombination between electrons and ions give rise to stellar photon emission and subsequent information about the temperature of the object. We note that the radiative recombination discussed above is the reverse of photoionization, a principle which has been frequently used to deduce photoionization cross sections from measurements of recombination light intensities. Once cross sections, spectral light fluxes, and densities and velocity distributions of all reactants in a plasma are known, the energy balance of the system can be studied.

Unfortunately, little information is available with respect to cross sections. Within the time limits of the present study it would

be impossible to investigate a high number of elements, and a decision was made to focus our attention on photoionization in cesium.

Cesium has been observed in our sun and in other stars[1], but the major justification for our work relies on the extensive use of the element, which has an ionization energy of only 3.89eV, in a number of devices, such as thermionic energy converters, ion and plasma propulsion engines, MHD generators, and lasers. Available experimental data and theoretical predictions show a wide scatter in absolute photoionization cross section values and even uncertainities as to the existence and importance of molecular cesium ions in electrical discharges. One result of the lack of quantitative data is that significant ionization processes in some cesium devices (particularly the ignited mode thermionic converter) are not yet known in sufficient detail.

Almost all experimental photoionization studies in the past have been limited to ground-state species. Photoionization from the excited state, however, can be significant in stellar atmospheres and in plasma devices containing high densities of excited states. Furthermore, the photoprocesses responsible for "smog" fall within the category of principles discussed in this report and can be studied at a later time with only slight modifications of the apparatus.

The objective of the present thesis has been to study the cross section for photoionization of excited cesium atoms. The specific reaction to be considered is the two step process:

$$Cs\ (6^2S_{1/2}) + h\nu_1 \rightarrow Cs^*\ (6^2P_{3/2,1/2}) \qquad (1)$$

$$Cs^*\ (6^2P_{3/2,1/2}) + h\nu_2 \rightarrow Cs^+ + e\ . \qquad (2)$$

The frequency ν_1 is fixed and represents the resonance radiation corresponding to wavelengths of 8521 and 8944 Å, respectively, whereas the frequency ν_2 of the ionizing radiation is variable, corresponding to light with wavelengths below the ionization threshold of 5060 Å. The cross section to be determined is for process (2) above.

The salient feature of the experiment is to use three crossed beams, i.e., two light beams intersecting a beam of cesium atoms. The ions produced are extracted in a direction perpendicular to the plane of the three beams and electrostatically focussed onto a CuBe dynode, where the secondary electrons produced are multiplied with a Channeltron to yield a countable pulse.

With an atomic beam density of 10^{10} cm^{-3}, an effective excitation light flux of 10^{15} cm^{-2} s^{-1}, and ionization light flux of 10^{14} cm^{-2} s^{-1}, we obtained a signal of approximately 10 counts per second. From an analysis of this count rate as a function of photon frequency we have derived the relative cross section for process (2) above. The cross section exhibits a sharp onset and maximum at 5060 Å, and appears to decrease faster with decreasing wavelength than do the results of Mohler and Boeckner[2]. Furthermore, our data appear to exhibit a minimum at 3000 Å, an effect which has not been theoretically predicted.

The material in this part of the dissertation is organized as follows: In Section B we present a detailed account of ionization

mechanisms in cesium which was deemed necessary for a deeper understanding of the many undesired background phenomena that occurred during the experimental phase. Then, in Section C, we discuss theories of photoionization in the alkali elements, with special emphasis on cesium. The experimental approach used during this investigation is characterized by a number of novel features, and is described and compared with other methods in Section D. The results and their interpretation as well as a complete discussion of consistency checks and background effects are found in Section E. Finally, in Section F we present conclusions and plans for continuation of this research.

B. IONIZATION MECHANISMS IN CESIUM

Ionization processes leading to the production of atomic ions can be conveniently divided into groups, depending on whether the ionizing agent is an electron or a photon. For electron impact we have

$$Cs + e \rightarrow Cs^+ + 2e \tag{3}$$

and

$$Cs^* + e \rightarrow Cs^+ + 2e \ . \tag{4}$$

The cross section for reaction (3) has been studied experimentally by McFarland and Kinney[3], Heil and Scott[4], Korchevoi and Przonski[5] and, most recently, by Nygaard[6]. No measurements have been made of the electron impact ionization of Cs* (reaction (4)) although an investigation of this cross section is in progress in our laboratory.

Similarly, possible photoionization processes are

$$Cs + h\nu \rightarrow Cs^+ + e \tag{5}$$

and

$$Cs^* + h\nu \rightarrow Cs^+ + e \quad . \tag{6}$$

A compilation of experimental and theoretical results[7-12] for reaction (5) is shown in Fig. (1). The experimental scatter is large and more data are needed. There is also significant disagreement among the theoretical calculations.

Because the reverse of reaction (6) is radiative recombination to an excited state of the neutral atom, the photoionization cross section from an excited state can be found from recombination measurements in a cesium electrical discharge, using the principle of detailed balancing in analyzing the data. Results of such indirect measurements of and theoretical calculations[2,12-16] for the excited state photoionization cross sections are shown in Fig. (2). A more comprehensive review of the theoretical and experimental methods that have been applied to this process is contained in parts C and D of this report.

Whenever excited atoms exist in large concentrations, they may collide and form molecular ions. The following schemes have been studied by other authors:

$$Cs\ (6P) + Cs\ (6P) \rightarrow Cs_2^+ + e \tag{7}$$

$$Cs\ (nP) + Cs\ (6S) \rightarrow Cs_2^+ + e \quad , \tag{8}$$

where, in reaction (8), $n \geq 8$. The process involving two cesium atoms in the 6P state was first found by Freudenberg[16] in 1931; later studies have been performed by Pollock and Jensen[17] and by Kniazzeh[18]. The latter investigator found the cross section to be $(7\pm5) \times 10^{-18}$ cm^2. In reaction (8) an atom in state 8P or higher is colliding with a

FIGURE 1

PHOTOIONIZATION CROSS SECTION FOR GROUND STATE CESIUM. Curve (B&D) represents absolute measurements of Braddick and Ditchburn[8]. The relative measurements of Mohler and Boeckner[7] (M&B) and Lawrence and Edlefsen[9] (L&E) have been normalized to (B&D) at 3130 Å. The curve (B&S) has been calculated, by Moskvin[13], from the quantum defect method of Burgess and Seaton[11]. The (B&S) results adjusted to Stone's[27] oscillator strengths give the curve (N&S) as calculated by Norcross and Stone[14]. Curve (W) shows the results of a calculation by Weisheit[12] which explicitly includes core polarization. Recent absorption measurements by Creek and Marr are presented as curve (C&M). On this figure all theoretical results are shown as dashed curves, while experimental results are drawn with solid lines.

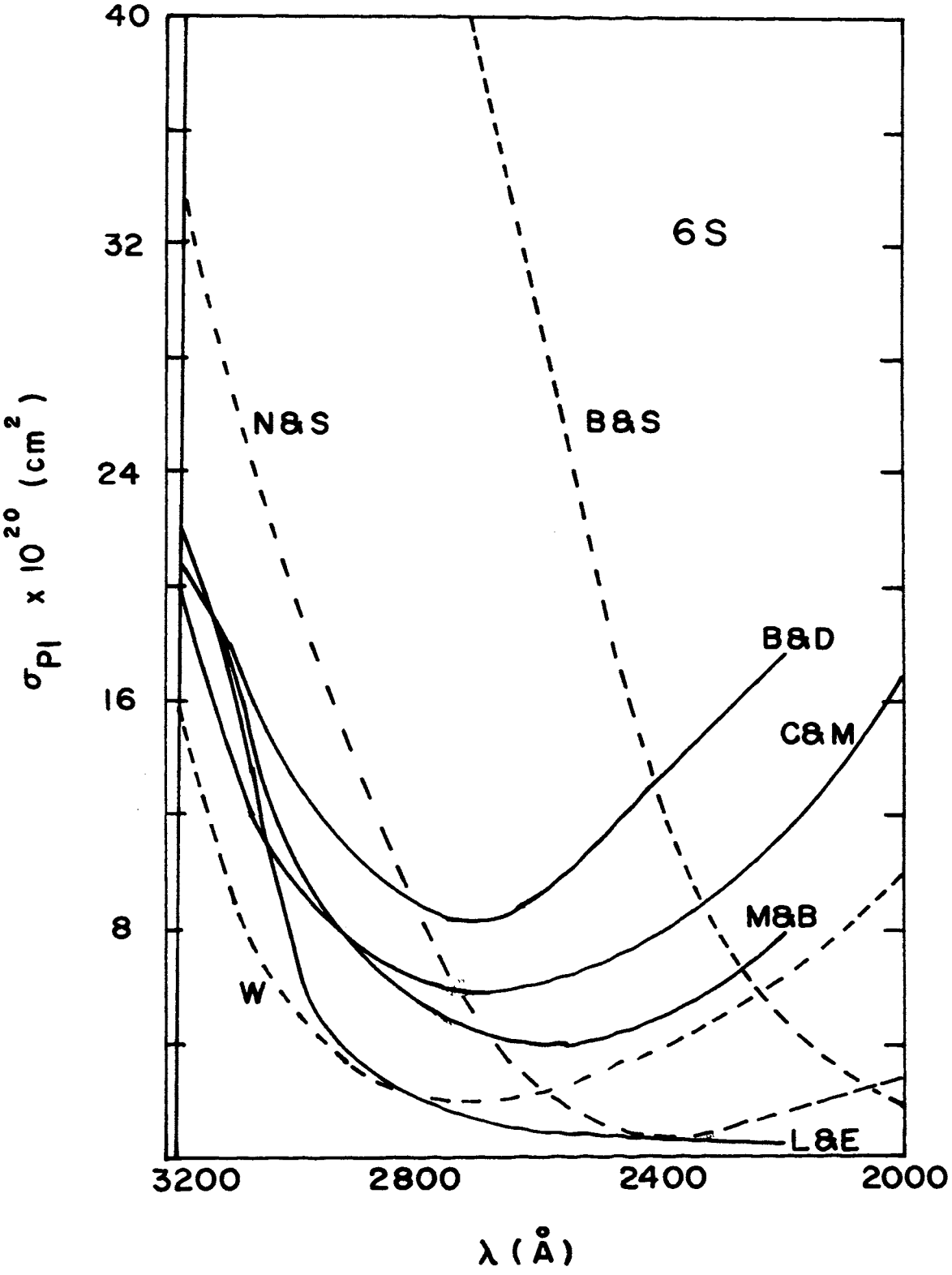
40
32
24
16
8
σ_{PI} x 10^{20} (cm^2)
6S
N&S
B&S
B&D
C&M
M&B
W
L&E
3200
2800
2400
2000
λ (Å)

Fig. 1

FIGURE 2

PHOTOIONIZATION CROSS SECTION OF CESIUM FROM THE 6P STATE. Experimental curves (solid lines) are from the recombination cross section measurements of Agnew and Summers[15] (A&S) and of Mohler and Boeckner[2] (M&B). Theoretical curves (dashed lines) are a direct calculation using the quantum defect method by Moskvin[13] (M) and the adjusted quantum defect method of Norcross and Stone[14] (N&S).

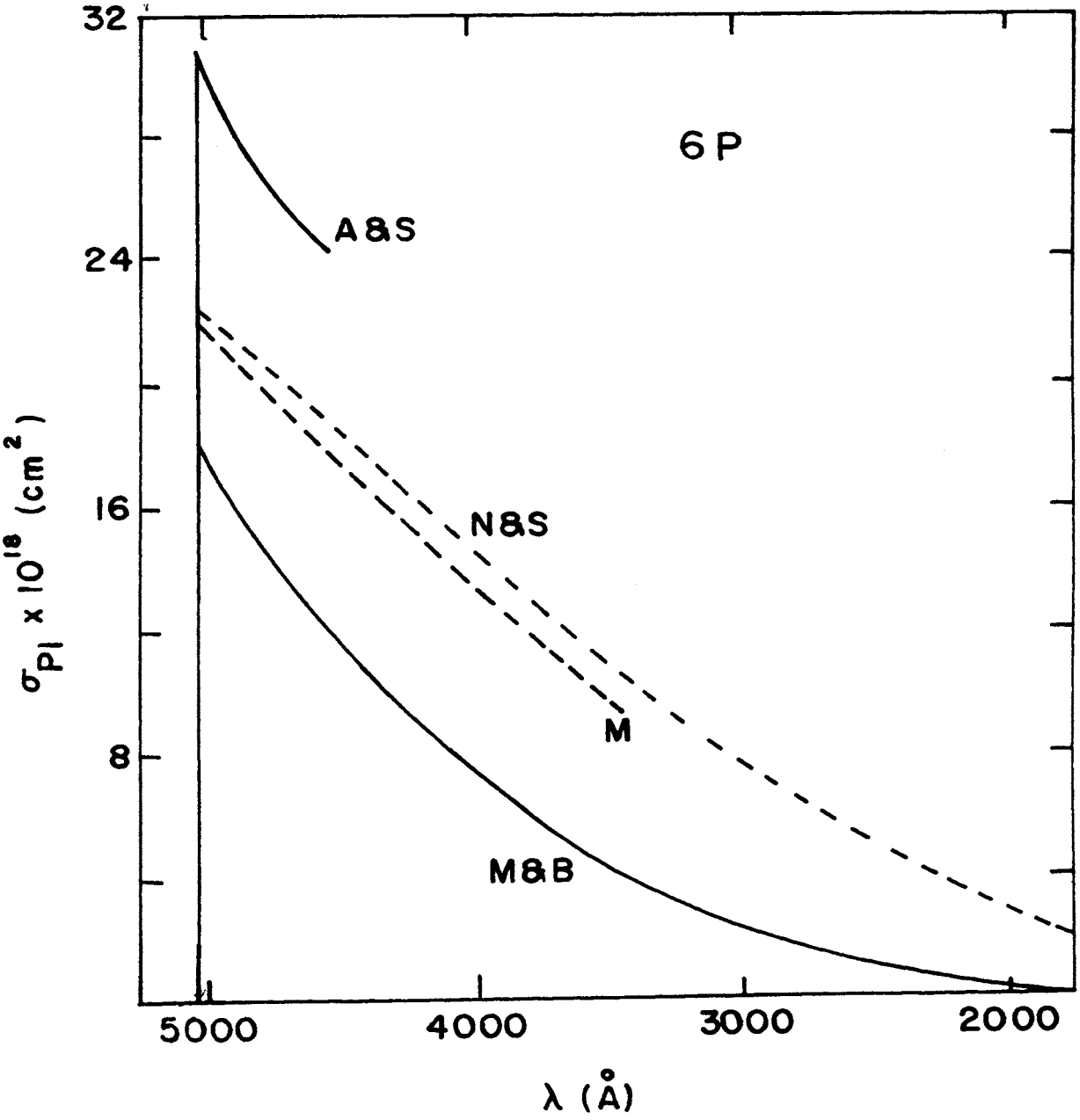

Fig. 2

ground state atom. The resulting molecular ion production has been studied by Mohler and Boeckner[19], Lee and Mahan[20], and Popescu et al.[21]

C. THEORY

In this section a brief review of the approaches that have been used to theoretically calculate the photoionization cross section for cesium is presented.

The photoionization cross section at a frequency ν for an atomic system is given by[22]

$$\sigma_{n\ell}(\nu) = \frac{\pi e^2 h}{mc} \sum_{\ell'=\ell\pm1} \frac{d f_{n'\ell', n\ell}}{dE} , \tag{9}$$

where $f_{n'\ell', n\ell}$ is the oscillator strength of the transition from a bound state $n\ell$ to an accessible state in the continuum. The oscillator strength has the standard definition, i.e.[22],

$$f_{n'\ell', n\ell} = \frac{4\pi m}{h} \omega_{n'\ell', n\ell} \left| \langle n'\ell' | e\vec{r} | n\ell \rangle \right|^2 , \tag{10}$$

where $\omega_{n'\ell', n\ell}$ is the frequency of the photon absorbed by the atom in making the transition from the bound state $n\ell$ to the continuum state $n'\ell'$. The other symbols have their standard meanings.

It should be noted that the majority of available theoretical calculations in the alkalies limit themselves to lithium for reasons of simplicity. The most recent calculation and an excellent critical review of the methods that have been used to calculate lithium photoionization cross sections have been performed by McDowell[23]. A complete discussion of all of the basic approaches that have been employed is discussed by Marr[24].

Basically, two different approaches have been successfully applied to calculating photoionization cross sections in cesium. The first of these is the quantum defect method (QDM) which was first developed by Seaton[25] in the context of photoionization. This method assumes that the neutral cesium atoms obey the Schroedinger equation of the form

$$\left[-\frac{h^2}{2m}\left(\frac{d^2}{dr^2} - \frac{\ell(\ell+1)}{r^2} \right) - V(r) + E \right] Y(E,\ell,r) = 0 \quad . \qquad (11)$$

The bound state wavefunctions are constructed to predict the correct energy level spectrum. The free state wavefunctions are essentially plane wave solutions. For bound-free transitions the quantum defect method yields the matrix element

$$|\langle n'\ell'|r|n\ell\rangle|^2 = g^2(n'\ell',n\ell)$$

where

$$g(n'\ell',n\ell) = \eta^2 L^{-1/2}(\eta,\ell)G(n'\ell',n\ell)\cos\pi[\eta + \mu_\ell(\eta) + \chi(n'\ell',n\ell)]. \qquad (12)$$

The effective quantum number η is defined by

$$\frac{e^2}{2a_0\eta^2} = E_{n\ell}$$

and the quantum defect is defined by

$$\mu_\ell(\eta) = n - \eta$$

Furthermore,

$$L(\eta,\ell) = 1 + \frac{2}{\eta^3}\frac{\partial\mu_\ell(\eta)}{\partial E}$$

which is approximately equal to unity for cesium. Burgess and Seaton[26] have tabulated the functions G and χ.

Using this formalism, Moskvin[13] calculated the photoionization cross sections from both the 6S and 6P states of cesium, as shown in Figs. (1) and (2).

Norcross and Stone[14] improved the quantum defect method by adding an adjustable parameter $\lambda_{\ell',\ell}(n)$ to the argument of the cosine in Eq. (12). The value of this parameter was chosen to bring the QDM oscillator strengths into best agreement with those calculated by Stone[27]. In this previous work he calculated oscillator strength using one-electron wave functions which were numerical solutions of the Schroedinger equation with a central symmetric potential and with the spin orbit term. The results of the Norcross and Stone calculations are also shown in Figs. (1) and (2).

The second approach, which to date has been applied only to ground state cesium, is to modify Eqs. (10) and (11) by including both core polarization and spin-orbit interactions. Core polarization is accounted for by replacing the dipole operator in Eq. (10) with[12]

$$e\vec{Q}(\vec{r}) = e\vec{r}\{1 - \alpha_d[1-\exp(-r/r_c)^3]/r^3\} \qquad (13)$$

where α_d is the static core dipole-polarizability and r_c is the effective core radius. The values of r_c are obtained from calculated bound-bound oscillator strengths compared to the most reliable experimental data.

The effect of spin orbit interactions is included by adding to the potential in Eq. (11) a term of the form

$$\frac{1}{2}\alpha^2 S(r)\vec{\ell}\cdot\vec{s} \quad ,$$

where α is the fine structure constant and S(r) is a radial function

whose value is chosen to reproduce the P-state fine-structure energy defects.

D. EXPERIMENTAL ARRANGEMENT

1. Introductory Remarks

This experiment is the first attempt to directly measure the photoionization cross section from a short-lived excited atomic state prepared in a beam of neutral atoms.

The advantages of cross-beam experiments with reference to photodissociation of negative ions have been discussed by Branscomb[28]. To the author's knowledge, the only direct photoionization measurement from a pre-selected state was performed by McNeal and Cook[29] in a flowing afterglow in nitrogen. The flowing afterglow technique cannot be used in the present experiment because the lifetime of the excited state is only 30 ns.

Previous to this work photoionization cross sections in cesium had been determined in two different ways[30]. The first of these is a straightforward transmission experiment which has been used by a number of workers to study photoionization from the ground state of cesium. In this type of experiment the spectrum of an ultraviolet light source is recorded on a photographic plate. Cesium vapor is then introduced into the optical path and a new spectrum is recorded. The cross section is determined from the defining relation

$$\log \frac{I_0(\nu)}{I(\nu)} = \sigma(\nu) n_0 x \quad . \tag{14}$$

In this equation $I_0(\nu)$ is the incident light intensity, $I(\nu)$ is the transmitted light intensity, $\sigma(\nu)$ is the photoabsorption cross section, n_0 is the number density of cesium atoms, and x is the path length

through the cesium vapor. The problems associated with this type of an experiment are the determination of the cesium number density and its constancy over the optical path length and the effect of absorption by cesium dimers[31]. For these reasons and because fraction of absorbed photons is very small, the technique was judged infeasible for the present experiment.

A second approach, which has been used to determine the cross section for photoionization of both ground-state and excited cesium, is to study recombination radiation from a cesium plasma. Since the matrix elements for absorption and emission are equal, one can obtain the photoionization cross section from the recombination coefficient if one knows the energy distribution of the electrons. The energy distribution is not accurately known due to the effects of inelastic collisions, thus introducing a major source of systematic error in this approach.

To avoid these difficulties, we performed a triple crossed-beam experiment, i.e., two light beams intersecting a beam of cesium atoms (see Fig. 3). One light beam was at an appropriate frequency to induce the transition

$$Cs\ (6S) + h\nu_1 \rightarrow Cs^*\ (6P_{3/2,1/2}) \ .$$

The second light beam was of an appropriate frequency to ionize the excited cesium,

$$Cs^*\ (6P_{3/2,1/2}) + h\nu_2 \rightarrow Cs^+ + e \ .$$

The strengths and weaknesses of crossed beam experiments have been summarized in a review article by Bederson and Kieffer[32] as follows:

> Atomic-beam techniques possess great potential versatility in regard to the preparation of selected species, velocities and states. Although conceptually

FIGURE 3

SCHEMATIC DIAGRAM OF THE EXPERIMENTAL APPARATUS USED TO DETERMINE THE PHOTOIONIZATION PRODUCTION RATE. Both the excitation and ionization radiation beams impinge on the atomic beam in the doubly illuminated area. The ions produced are extracted from the beam and detected with a Channeltron electron multiplier. The atomic beam density is monitored with a surface ionization detector (SID).

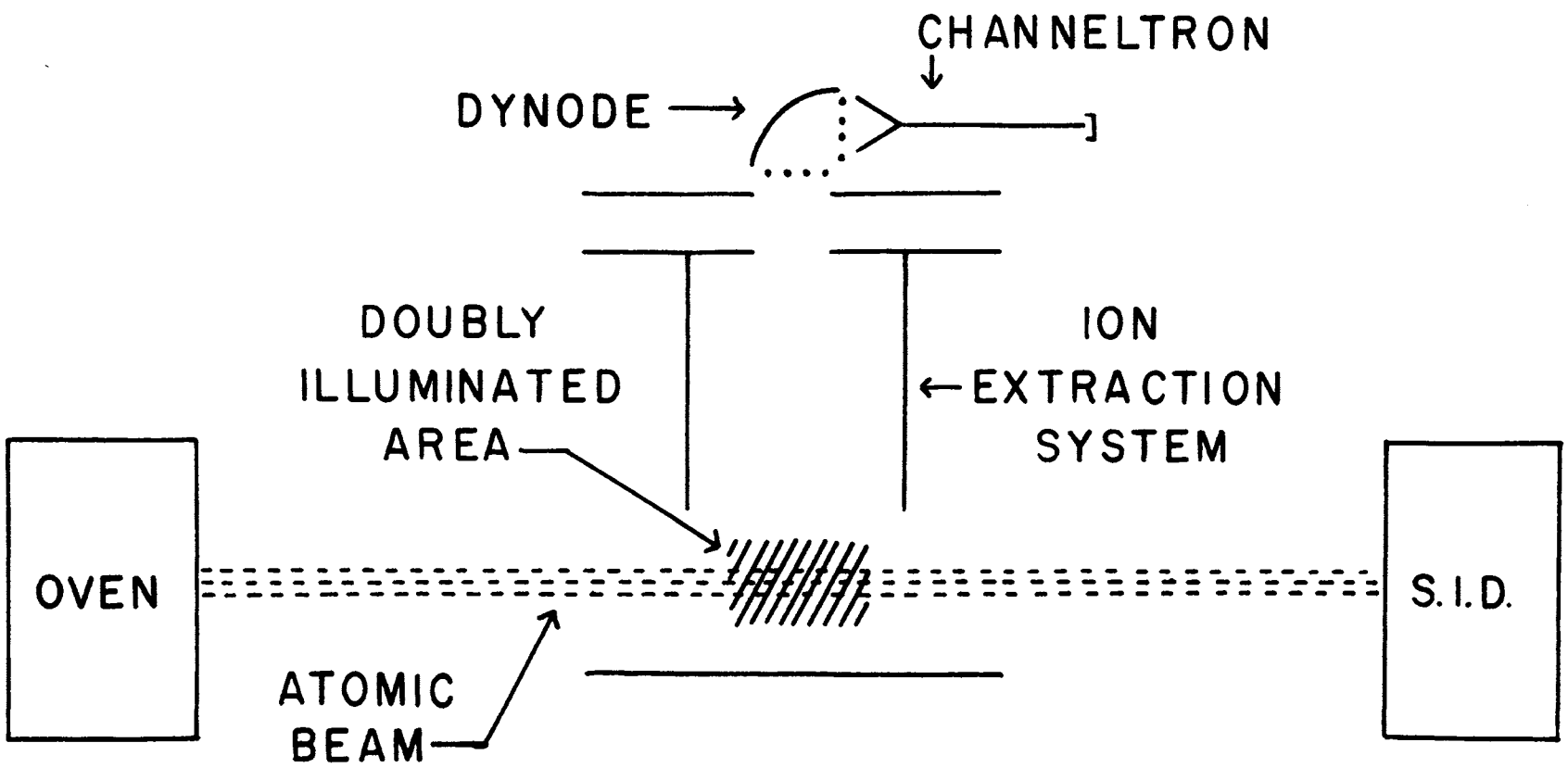
CHANNELTRON
DYNODE
DOUBLY
ILLUMINATED
AREA
ION
EXTRACTION
SYSTEM
OVEN
S.I.D.
ATOMIC
BEAM

Fig. 3

> simple, such experiments are often very difficult (and expensive) to perform in practice. Particularly when state selection, unstable species, or some other form of energy or state discrimination is employed, the signal-to-noise ratio, and in some cases the absolute signal itself, is quite unfavorable. Thus elaborate data averaging procedures must be employed simply to overcome the statistics. As a consequence, very limited use has been made of these crossed-beam capabilities in the past although this situation is now improving.

2. Atomic Beam

In this case, "to overcome the statistics," the data had to be accumulated for several hours so that care had to be observed in the design and construction of the atomic beam to insure long term stability. The atomic beam oven contained two chambers. The first consisted of an OFAC copper tube containing a glass ampule of cesium metal which was broken after the ultimate background chamber pressure, typically 10^{-9} torr, had been attained. The temperature of the liquid cesium was electrically controlled, thereby maintaining the cesium vapor number density constant to within ±2%. The second chamber was the oven proper, constructed of stainless steel and heated with a molybdenum filament to a temperature 25°C above the reservoir. The cesium atoms passed from this oven through a collimating hole structure (manufactured by Brunswich Corporation) consisting of 5500 holes, each with a diameter to length ratio of 1:20. After the beam passed through the interaction region, it was monitored with a surface ionization detector (SID). A typical result displaying the positive ion current as a function of SID tungsten filament temperature is shown in Fig. 4. An independent check on the proper operation of the apparatus is to measure the electron emission current from the hot filament in the

presence of the atomic beam as a function of the inverse filament temperature. (The temperature of the filament was determined from the tables of Jones and Langmuir[34].) The result is the characteristic Langmuir[35] S-curve, Fig. 5, from which we obtain a work function in the high temperature limit of about 5.3eV. This is consistant with a previous observation by Croft and Nygaard[33].

3. Production of Excited Atoms

One of the major difficulties in two-step photoprocesses is to generate and maintain a high concentration of excited atoms. We have used GaAs lasers, hollow cathode discharge lamps, and cesium rf lamps for the production of cesium atoms in the $6^2P_{3/2,1/2}$ -states. Although some preliminary work was done using hollow cathode lamps, intensity instabilities and limited lifetimes made them unsuitable for precise work. Furthermore, because GaAs lasers are extremely difficult to operate, in spite of the promising results in Appendices 1 and 2 of this report, the photoionization data presented here were obtained using a cesium rf lamp of the type developed by Franz[36]. Our lamp had a long-term stability of better than 5% which is in good agreement with his results. He obtained maximum output for a xenon buffer gas pressure of 1.5 torr, as compared to an optimal pressure of 0.8 torr in our version of the lamp. At maximum output it was observed that our lamp emitted with equal intensity, to within 10%, in each of the resonance lines.

Since the photoionization cross-section is directly proportional to the density of 6P atoms, it is in order to estimate this density.

FIGURE 4

POSITIVE ION CURRENT IN SURFACE IONIZATION DETECTOR AS A FUNCTION OF FILAMENT TEMPERATURE. The current plateau corresponds to an atomic beam density of 5×10^{11} cm^{-3}.

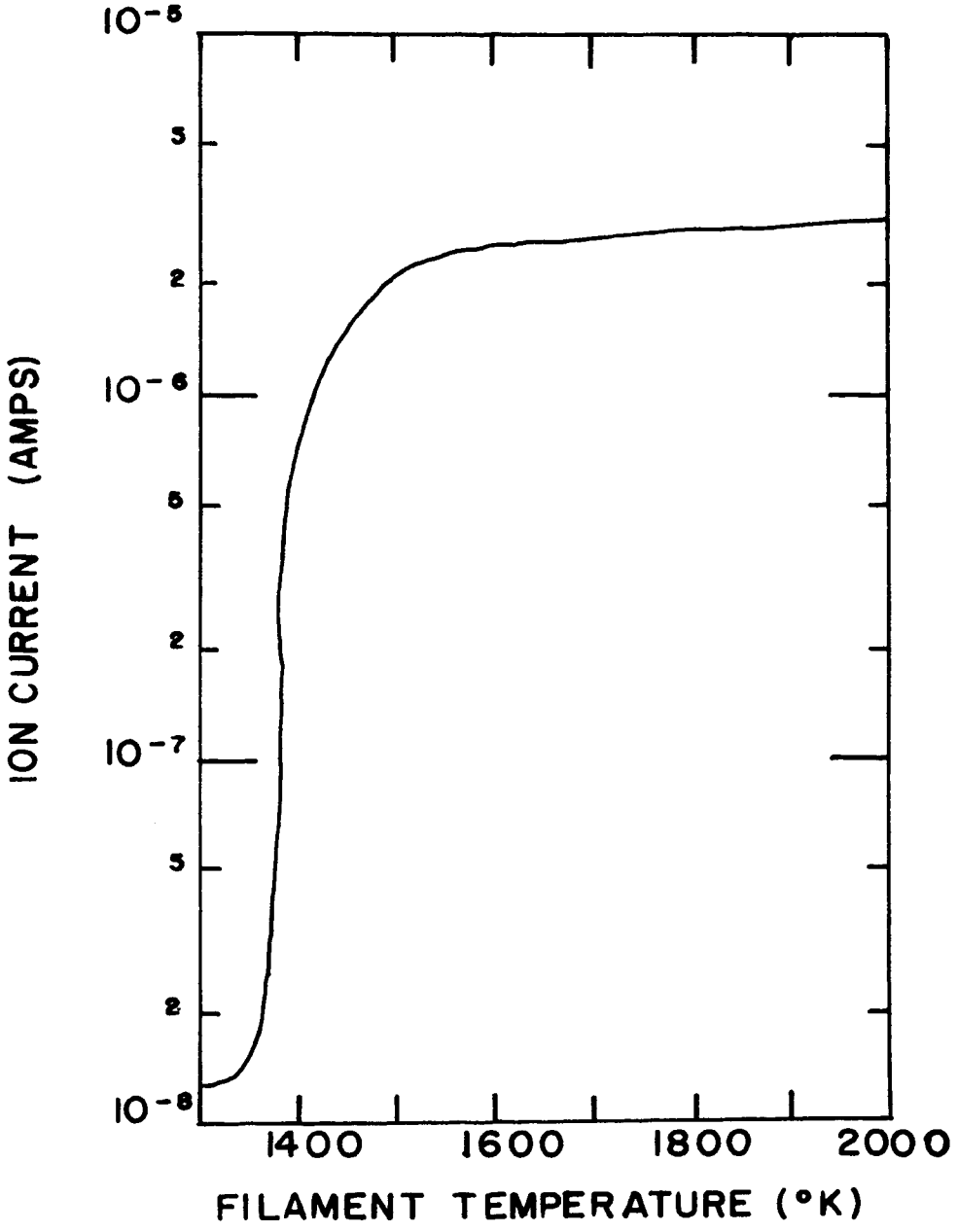
ION CURRENT (AMPS)
10⁻⁵
5
2
10⁻⁶
5
2
10⁻⁷
5
2
10⁻⁸
1400
1600
1800
2000
FILAMENT TEMPERATURE (°K)

Fig. 4

FIGURE 5

FILAMENT ELECTRON EMISSION CURRENT AS A FUNCTION OF INVERSE TEMPERATURE. During the measurement the filament was exposed to a beam of cesium atoms of density 5×10^{11} cm^{-3}. The filament was a 7 mil tungsten wire, 2 cm long.

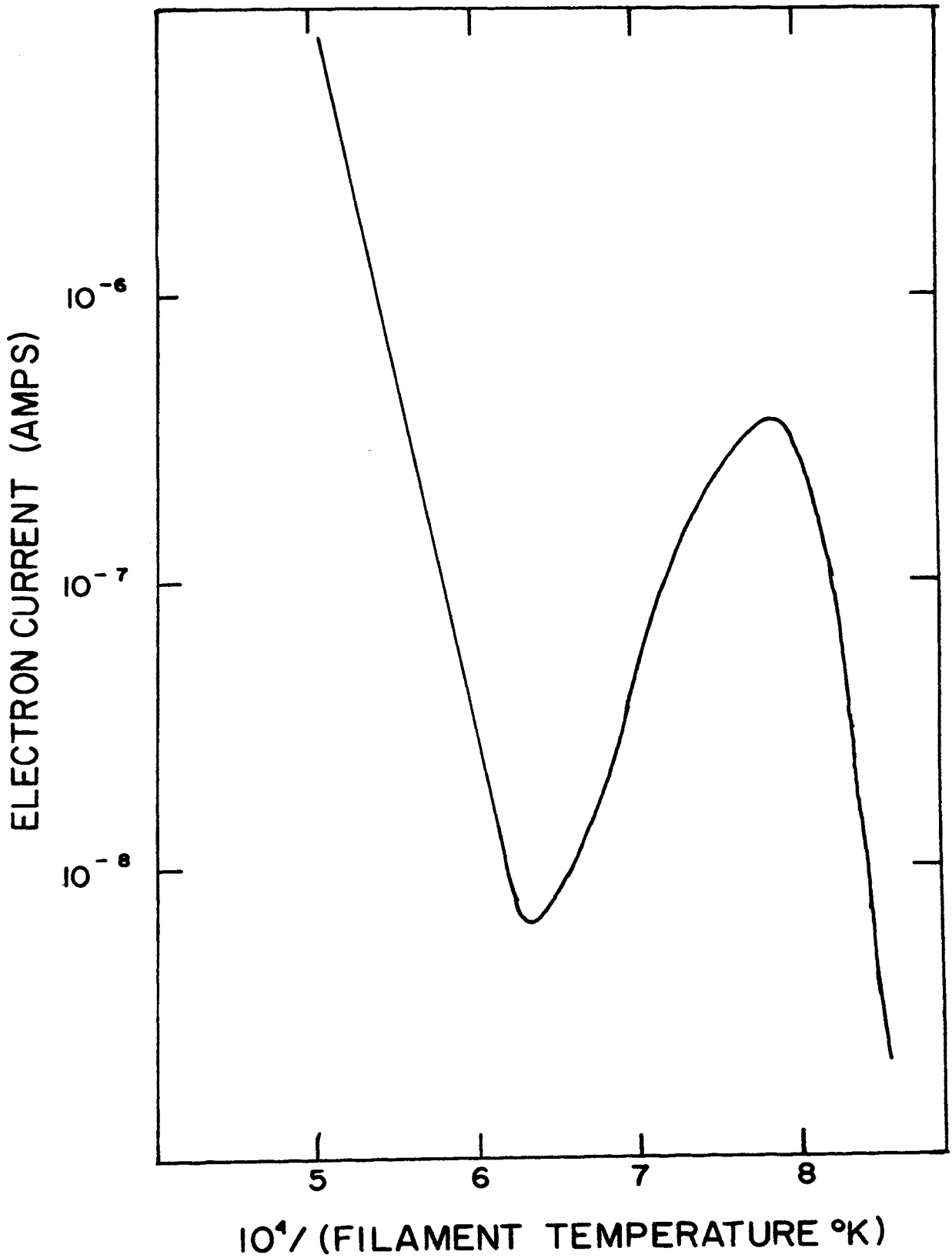
ELECTRON CURRENT (AMPS)
10⁻⁶
10⁻⁷
10⁻⁸
5
6
7
8
10⁴/ (FILAMENT TEMPERATURE °K)

Fig. 5

We note that the number of photons of wavelength λ_0 transmitted through an atomic beam of thickness ℓ is

$$j(\ell) = j_1 e^{-K_0 \ell} , \tag{15}$$

where j_1 is the incident flux of photons and K_0 is the absorption coefficient of the atomic beam.

If the interaction volume is $V = A\ell$, the number of photons absorbed per cm^3 per second is $(j_1/\ell)[1-\exp(-K_0\ell)]$. The rate equation for the density of 6P atoms is then

$$\frac{dn^*}{dt} = - \frac{n^*}{\tau} + \frac{j_1}{\ell} \left[1-e^{-K_0 \ell} \right] . \tag{16}$$

In steady state, this can be solved to yield

$$n^* = \tau \left(\frac{j_1}{\ell} \right) \left(1-e^{-K_0 \ell} \right) . \tag{17}$$

For pure Doppler broadening, K_0 has the form

$$K_0 = \frac{2}{\Delta\nu_D} \left(\frac{\ell n^2}{\pi} \right)^{1/2} \frac{\lambda_0^2}{8\pi} \frac{g_2}{g_1} \frac{n_0}{\tau} \tag{18}$$

where λ_0 is the center wavelength, g_2/g_1 is the ratio of the statistical weights of the two states (2 in this case), and $\Delta\nu_D$ is the spectral absorption width of the beam. Another fact that must be taken into consideration is that the width of the line emitted by the lamp is about a factor of 10 larger than the absorption line. So to obtain an order of magnitude estimate for n* let us define an effective light flux

$$j_{1,eff} \equiv \frac{\Delta\nu_D}{\Delta\nu_E} j_1$$

and rewrite Eq. (17) as

$$n^* = \tau \, (j_{1,eff}/\ell) \quad 1\text{-}e^{-K_0 \ell} \quad . \tag{19}$$

In this experiment, the following numbers and estimates prevail:

$\tau = 30 \times 10^{-9}$ s

$j_{1,eff} = 10^{15}$ cm^{-2} s^{-1}

$K_0 \ell = 0{,}1$

These numbers inserted into Eq. (19) give $n^* \simeq 2 \times 10^6$ cm^{-3} as compared to $n_0 = 10^{10}$ cm^{-3}.

4. Ion Production and Detection

The number of ions produced per cm^3 per second as a result of two-step photoionization can be written as

$$\frac{dn^+}{dt} = n^* \sigma j_2 \quad , \tag{20}$$

where σ is the cross section for photoionization of the 6P-atoms and j_2 is the flux of ionizing photons. Assuming an interaction volume of 0.1 cm^3 and a cross section of 6×10^{-18} cm^2, the number of ions produced per second is

$$N^+ = \frac{dn^+}{dt} V \simeq 10^{-13} j_2 \quad . \tag{21}$$

Typically, with $j_2 = 10^{15}$ cm^{-3} sec^{-1}, count rates of the order of 100 per second are expected. The observed count rate was of the order of 10 per second.

Two different light sources were used to produce the ionizing radiation. One was a 250W Hg lamp which produced a set of discrete, strong lines, superimposed on a continuum in the wavelength region

from 5000 - 2000 Å. The other was a 250W quartz-tungsten-iodine lamp which yielded an intense continuum centered about 5000 Å, thus overlapping the important threshold region of the photoionization cross section. The specific lines of interest were isolated with narrow band interference filters or with a 0.25 m grating monochromator. The ions produced were extracted from the interaction region, accelerated to an energy of 3KeV and focussed onto a CuBe dynode. The secondary electrons thus produced were amplified with a Channeltron electron multiplier to yield a countable pulse.

Cesium, being a conductor, would drastically modify the potential distribution of the ion focussing system if it were allowed to deposit on ceramic insulators separating the various components. To guard against this eventuality, the entire system was surrounded with a copper surface that was in intimate contact with a liquid nitrogen reservoir.

5. Electronic Apparatus

Some rather complex data handling techniques had to be employed to extract the signal from background effects. A block diagram of the pulse handling circuitry is shown in Fig. 6. The negative pulses emitted from the Channeltron are amplified, inverted, and fed into a discriminator which delivers one 10 volt pulse for each sufficiently large input pulse. The discriminator level is set so that the background count rate is much less than one count per second when the ion extraction system is off. This portion of the circuitry is capable of handling a maximum count rate of 10^6 pulses per second.

FIGURE 6

BLOCK DIAGRAM OF PULSE HANDLING APPARATUS. All pulses are drawn with positive potential upward.

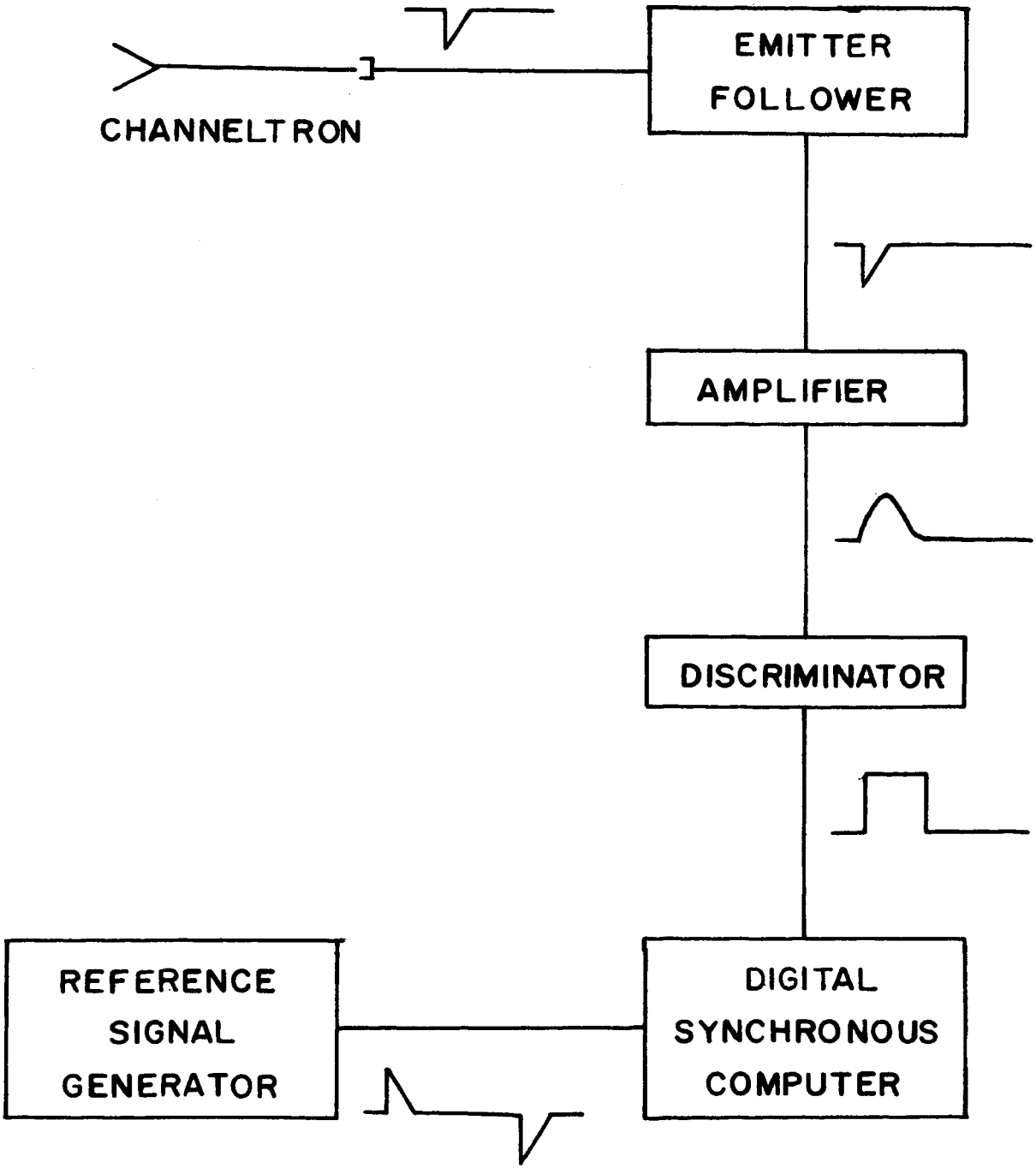
CHANNELTRON
EMITTER FOLLOWER
AMPLIFIER
DISCRIMINATOR
REFERENCE SIGNAL GENERATOR
DIGITAL SYNCHRONOUS COMPUTER

Fig. 6

The timing signal needed for the digital synchronous computer[37] is derived from a mechanical chopper placed in the path of the exciting light beam. For clarity let us define "on" as the condition in which the exciting light beam is intersecting the atomic beam and "off" as the condition in which the chopper wheel has blocked the exciting light beam. The reference signal generator emits a positive spike as the exciting light is turned on and a negative spike as it is turned off. The digital synchronous computer then is operated in the following manner. The positive spike opens one internal scaler, for a preset amount of time, typically 1.7×10^{-3} s. Similarly, the negative spike gates open a second scaler for an identical amount of time. In this way, the scaler that accumulates when the exciting light is on (positive spike) counts signal plus noise, and the one that accumulates when the exciting light is off (negative spike) counts only noise. After a preset number of chopper cycles, the two scaler readings are subtracted to yield the net signal count rate.

E. RESULTS AND DISCUSSION

Values for the relative cross section have been obtained at a number of discrete points in the wavelength region between 5000 Å and 2500 Å (Fig. 7). These results have been normalized to those of Mohler and Boeckner[2] at 4358 Å.

To insure that the photoionization cross section for photoexcited cesium was actually being obtained, we measured the ion count rate above the ionization threshold of 5060 Å and obtained zero ion counts, as indicated on the graph.

FIGURE 7

PHOTOIONIZATION OF CESIUM IN THE 6P STATE. The full drawn curve represents the recombination measurements of Mohler and Boeckner[2], while the present data points are represented by an "X". The present relative measurements have been normalized to those of Mohler and Boeckner at 4358 Å.

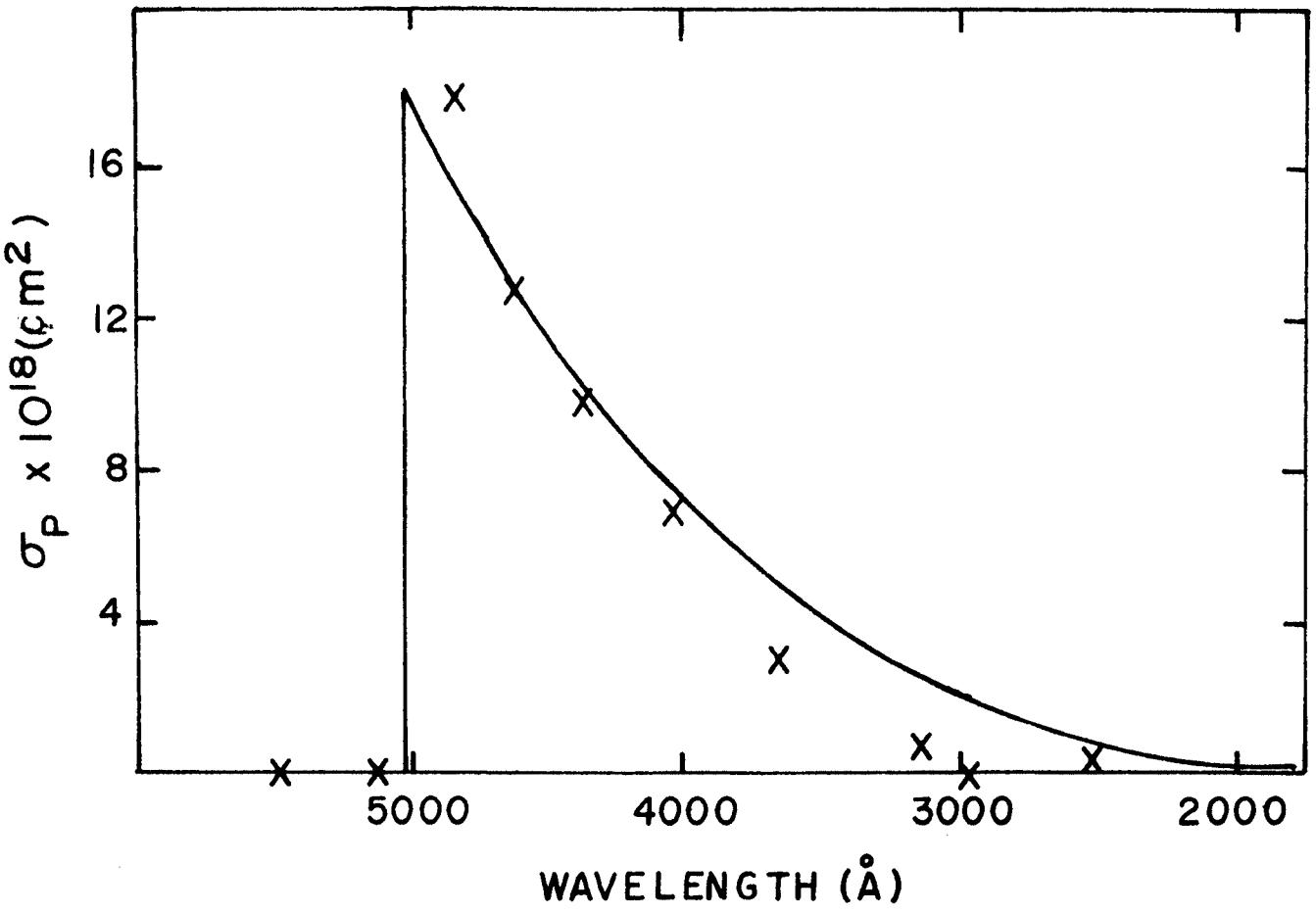
16
12
8
4
$\sigma_p \times 10^{18}(\text{cm}^2)$
5000
4000
3000
2000
WAVELENGTH (Å)

Fig. 7

We performed consistancy checks motivated by Eq. (20),

$$\frac{dn^+}{dt} = j_2 \, n^* \, \sigma \quad ,$$

from which we note that the count rate as recorded by the Channeltron and the electronics apparatus is

$$N = \eta V \frac{dn^+}{dt} = \eta V j_2 n^* \sigma \quad , \tag{22}$$

where η is an overall efficiency factor and V is the interaction volume. If one then expands the exponential in Eq. (17) and replaces K_0 using the expression

$$K_0 \, (\Delta\nu_D) = \pi \, r_0 \, c \, n_0 \, f_{6S-6P} \quad ,$$

where n_0 is density of ground state cesium atoms, r_0 is the classical radius of an electron and f_{6S-6P} is the excitation oscillator strength, and inserts that value for n* into Eq. (22), one obtains

$$N = \frac{\pi e^2}{mc} \tau \, f_{6S-6P} \, \eta \, V \, \sigma \, (j_1 \, j_2 \, n_0) \tag{24}$$

The quantities in parentheses j_1, j_2, n_0 are under the control of the experimenter, and the count rate should be directly proportional to each of them. We varied j_1 and j_2 by inserting neutral density filters in the light beams and the cesium number density n_0 by adjusting the reservoir temperature. In all cases it was found, to within ± 10%, that the count rate was indeed directly proportional to these quantities.

The data presented appears to decrease more rapidly with frequency than the recombination data. There also appears to be a minimum in the cross section in the neighborhood of 3000 Å. It should be noted however that even though each data point is the average of three to six twelve hour runs, the statistical deviation of the individual runs

is of order ± 10%. Furthermore it is possible that systematic errors could add another ± 10% to the overall error at each point. Taking account of these facts it is recognized that the present experiment does not unambiguously show that the previous measurements are incorrect. The present experiment does show, however, that it is possible to directly determine the relative photoionization cross section from a short lived, preselected, excited, atomic state and that further experimental effort in this direction is warranted.

The absolute calibration of the apparatus requires more time than was available for its inclusion in this report, but is presently in progress in our laboratory. The factors which must be considered for absolute calibration can be identified from an analysis of Eq. (22). To determine the cross section absolutely one must know the count rate, the overall efficiency of the detection system, the interaction volume, the intensity of the ionizing radiation, and the density of atoms in the excited state. To determine the efficiency of the detection system a known ion current must be introduced into the interaction region and these ions must be extracted and counted. The performance of this measurement requires a substantial modification of the present apparatus. This is the major reason why the present data must be presented as relative data only.

In the remainder of this section we shall discuss a number of background effects that made the experiment extremely difficult to carry out. The discussion relies heavily upon the treatment of ionization mechanisms in cesium presented in Section B. As a result of our analysis we have found that all undesired volume and surface effects are discriminated against by the modulation of the exciting

light, thus lending confidence to the relative cross section depicted in Fig. 7.

The primary competing processes and their effect on the experiment are discussed in the following paragraphs:

a. $Cs + h\nu_2 \rightarrow Cs^+ + e$

The direct photoionization of ground state cesium atoms occurs only for wavelengths below 3184 Å. Below this wavelength it is discriminated against by modulation of the exciting light beam.

b. $Cs^* + Cs^* \rightarrow Cs_2^+ + e$

This process was studied experimentally by extinguishing the ionizing light while keeping only the exciting light on. We found a zero count rate within the statistical limits, and can therefore neglect this process.

c. $Cs_2 + h\nu \rightarrow Cs_2^+ + e$

This effect has been noted by other workers[38,39], and in those cases its contribution to the total count rate was approximately 1%. We made no attempt to isolate this effect because it depended upon the intensity of the ionizing light alone and so was discriminated against by our modulation technique.

d. Cesiated Surface + $h\nu \rightarrow Cs^+$

Photoionic emission from cesiated surfaces at room temperature is a controversial issue. Medicus and Breaux[40] have presented evidence in support of this process, but their analysis has been criticized by Shaw and Stickney[41]. An attempt was made to measure the wavelength dependence of this effect, but in our apparatus this process can not be distinguished from process e, (to be discussed next) so no unambiguous conclusion can be drawn. Fortunately, in the actual

experiment this process is also discriminated against by the modulation scheme.

e. Cesiated Surface + $h\nu \rightarrow e$
e + Cesiated Surface $\rightarrow Cs^+$

This two-step sequence appears to be a major contribution to the noise count in this experiment. It starts with a photoelectron being emitted from a cesiated stainless steel surface somewhere in the ion extraction system. The electron is accelerated downward (see Fig. 3), producing ions within the atomic beam and at the cesiated bottom plate. The ion is then accelerated up the ion extraction system and is counted. This process is successfully discriminated against, however, by our modulation scheme.

f. $Cs + h\nu_2 \rightarrow Cs^*$
$Cs^* + h\nu_1 \rightarrow Cs^+ + e$

This process is essentially excitation by the ionizing radiation followed by ionization by the exciting light. It is automatically discriminated against by the cesium atom which allows only certain 6S-nP transitions. These transitions are well known and have been avoided.

g. Photoelectric Effect

Counts produced by scattered radiation hitting the CuBe surface or the Channeltron cone are again dependent only on the ionizing light beam so they are not counted as signal counts.

F. CONCLUSIONS

Since two-step ionization mechanisms often lead to significant ionization rates in a number of cesium-plasma devices, the objective of this thesis has been to study one of these processes, namely photoionization of excited cesium atoms.

The experimental arrangement comprises a combination of an atomic beam being intersected by two light beams. For excitation of the atoms to the $6^2P_{3/2,1/2}$-states a conventional rf discharge lamp was used. As an alternative optical pumping source we developed a technique based on the thermal tunability of GaAs lasers. Once a substantial concentration of excited atoms is produced, they are exposed to an intense flux of ultra-violet light. The ions produced as a result of the latter step are finally counted with a Channeltron.

The cross section for photoionization of cesium 6P -atoms was measured from threshold (5060 Å) to about 2500 Å. The results have been very encouraging in that no ions were detected for wavelengths of the ionizing radiation above 5060 Å. The cross section appears to have a maximum at threshold with magnitude of order 10^{-17} cm^2. It subsequently decreases toward shorter wavelengths, but at a faster rate than previously observed. The results of Mohler and Boeckner, with which we are making comparison, were obtained indirectly from a measurement of recombination light from a cesium plasma, whereas the present approach represents the first direct measurement of the cross section from a pre-selected, short-lived atomic state.

Further work is in progress in our laboratory to calibrate the apparatus to a higher degree of accuracy, and once this is completed, additional research will be conducted in the remaining alkali and alkaline earth elements. This program can yield experimental values of photoionization cross sections which both will be useful in the calculation of radiation transport properties and can be used for critical evaluation of theoretical calculations of these cross sections.

BIBLIOGRAPHY

1. G. Stellmachev, Astrophys Letters (G.B.) 3, 99 (1969).

2. F.L. Mohler and C. Boeckner, Bur. Standards J. Res., 5, 51 (1930).

3. R.H. McFarland and J.D. Kinney, Phys. Rev. 137, A 1058 (1965). See also R.H. McFarland, Phys. Rev. 159, 20 (1967).

4. H. Heil and B. Scott, Phys. Rev. 145, 279 (1966).

5. Yu. P. Korchevoi and A.M. Przonski, Soviet Phys. - JETP 24, 1089 (1967).

6. K.J. Nygaard, J. Chem. Phys. 49, 1995 (1968).

7. F.L. Mohler and C. Boeckner, Bur. Standards J. Res., 3, 303 (1929).

8. H.J.J. Braddick and R.W. Ditchburn, Proc. Roy. Soc. (London), 143, 472 (1934).

9. E.O. Lawrence and N.E. Edlefsen, Phys. Rev. 34, 233 (1929).

10. M.J. Seaton, Proc. Roy. Soc. (London), 208A, 418 (1951).

11. A. Burgess and M.J. Seaton, Mon. Not. Roy. Astron. Soc., 120, 121 (1959).

12. J.C. Weisheit, private communication (1971). For a description of the theoretical method applied to potassium see J.C. Weisheit and A. Dalgarno, Phys. Rev. Letters 27, 701 (1971).

13. Yu. V. Moskvin, Optics and Spectroscopy, 15, 316 (1963).

14. D.W. Norcross and P.M. Stone, J. Quant. Spectrosc. Radiat. Transfer 6, 277 (1966).

15. L. Agnew and C. Summers, Proc. VII Int. Conf. on Phenomena in Ionized Gases, Belgrade (1965).

16. K. Freudenberg, Z. Physik 67, 417 (1931).

17. D.H. Pollock and A.O. Jensen, J. Appl. Phys. 36, 3184 (1965).

18. A.G.F. Kniazzeh, Report on Twenty-Sixth Annual Conference on Physical Electronics (MIT, Cambridge, Massachusetts, 1966), p. 1.

19. F.L. Mohler and C. Boeckner, Bur. Standards J. Research 5, 51 (1930).

20. Y.T. Lee and B.H. Mahan, J. Chem. Phys. 42, 2893 (1965).

21. I. Popescu, A. Ghita, A. Popescu, and G. Musa, Ann. Physik 18, 103 (1966).

22. H.A. Bethe and E.E. Salpeter, Quantum Mechanics of One and Two Electron Atoms, Academic Press, Inc., New York 299f, (1957).

23. M.R.C. McDowell, Case Studies in Atomic Physics, North Holland Publishing Company, Amsterdam, Ch. 2 (1970).

24. G.V. Marr, Photoionization Processes in Gases, Academic Press, Inc., New York (1967).

25. M.J. Seaton, Proc. Roy. Soc. (London) 208A, 418 (1951).

26. A. Burgess and M.J. Seaton, Mon. Nat. Roy. Astron. Soc. 120, 121 (1959).

27. P.M. Stone, Phys. Rev., 127, 1151 (1962).

28. L.M. Branscomb, Atomic and Molecular Processes, Academic Press, Inc., New York, p. 100 (1962).

29. R.J. McNeal and G.R. Cook, VII International Conference on the Physics of Electronic and Atomic Collisions, p. 160 (Amsterdam, 1971).

30. For a recent review of photoabsorption cross sections see R.D. Hudson and L.J. Kieffer, Atomic Data 2, 205 (1971) and R.D. Hudson, Rev. Geophys. Space Phys. 9, 305 (1971).

31. D.M. Creek and G.V. Marr, Proc. Roy. Soc. A304, 233 (1968).

32. B. Bederson and L.J. Kieffer, Rev. Mod. Phys. 43, 601 (1971).

33. W.J. Croft and K.J. Nygaard, J. Sci. Instr. (J. Phys. E) 2, 1012 (1969).

34. H.A. Jones and I. Langmuir, Gen. Elec. Rev. 30, 310 (1927).

35. J.B. Taylor and I. Langmuir, Phys. Rev. 44, 423 (1933).

36. F.A. Franz, Rev. Sci. Instru. 34, 589 (1963).

37. Manufactured by SSR, Inc., Palo Alto, Calif.

38. M. Lubell and W. Raith, Phys. Rev. Letters 23, 211 (1969).

39. J. Kessler and J. Lorenz, Phys. Rev. Letters 24, 87 (1970).

40. O.P. Breaux and G. Medicus, Phys. Rev. Letters 16, 392 (1966).

41. M.L. Shaw and R.E. Stickney, loc. cit. 18, 824 (1967).

VITA

Robert Eugene Hebner, Jr. was born on February 11, 1945, in Minneapolis, Minnesota. He received his primary and secondary education in Victoria, Texas. He was graduated from St. Mary's University, San Antonio, Texas, with a Bachelor of Science degree in Physics in May 1967.

He has been enrolled in the Graduate School of the University of Missouri-Rolla since September 1967. In August 1969 he was awarded the degree of Master of Science in Physics.

APPENDIX I

SELECTIVE DEPOPULATION OF THE $6^2S_{1/2}$ (F=3) -LEVEL IN CESIUM

This material has been published in the Journal of the Optical Society of America 61, 1455 (1971).

Selective Depopulation of the $6^2S_{1/2}$ (F=3) -Level in Cesium*

Optical pumping of cesium in a room-temperature vapor cell has been accomplished by means of a pulsed gallium-arsenide laser. As the time-dependent laser frequency coincides with atomic transitions originating from the cesium groundstate hyperfine levels, light will be absorbed and thence re-emitted from the 6P-state. The hyperfine splitting between the F=3 and F=4 ground-state levels can easily be resolved with this method. The lowest hyperfine level has been selectively depopulated. On this basis the use of one or more GaAs lasers as a pumping source for cesium masers is indicated and discussed.

1.0. INTRODUCTION

A direct optical pumping method for cesium masers would offer an alternative to the magnetic deflection scheme that is presently utilized to separate cesium atoms into groups of F=3 and F=4 in atomic clocks[1]. Notable attempts in this direction have been proposed and discussed by Franz[2] and by Beaty et al.[3] The principle of Franz's scheme, which applies to both rubidium and cesium, is to depopulate the lowest alkali ground-state hyperfine level by (σ^+) D_1 ($^2S_{1/2} \rightarrow {}^2P_{1/2}$) resonance radiation. The addition of a heavy noble gas, such as Kr or Xe, to the absorption cell, controls the relaxation process by the formation of stable alkali noble gas molecules, thereby establishing the population inversion that is a prerequisite for maser action[4]. The other method, suggested by Beaty et al., is based on the proximity between the 8521.4 Å Ar line and the Cs resonance

line. If an argon discharge lamp is placed in a strong magnetic field of about 1 weber/m^2, the line will Zeeman-shifted in such a direction that overpopulation between the ground-state F=4 and F=3 hyperfine levels becomes feasible[4].

The objective of this article is to present a novel method for selective depopulation of the $6^2S_{1/2}$ (F=3) -level in cesium. The pumping source consists of a thermally tuned gallium-arsenide laser, and with this device we have succeeded in resolving the two ground-state hyperfine levels[5]. A natural extension of this observation is to study the feasibility of using GaAs lasers as a source of excitation in a Cs vapor-cell maser.

It is of interest here to compare the proposed GaAs laser - cesium cell maser with other alkali masers. Rubidium masers[6], for instance, have been constructed largely because of the serendipitous existence of two stable naturally occurring isotopies, Rb^{87} and Rb^{85}. One of these isotopes is used in both resonance lamp and maser cell. If now a vapor cell containing the other isotope is placed between the lamp and the maser cell, light corresponding to transitions from the upper hyperfine level of the S-state to the P-state is blocked and population inversion can be attained.

For cesium, because of the lack of an additional isotope, no such filter has been developed. The advantages of the proposed method are the absence of filters and magnetic field. We also note that the power output from a single GaAs laser junction is about one hundred to one thousand times higher than from a resonance lamp operating in the same wavelength region, although the very high power is not

necessary for maser action. More important is the property that the radiation is well filtered, the laser mode used for the pumping being separated from other laser modes by several Ångströms. The lasers can be operated in a pulsed or cw mode, and the frequency can be tuned to a given hyperfine transition within the atomic system.

The body of this paper is organized into three major sections: First, we discuss the characteristics of GaAs lasers with special emphasis on the principles and mechanisms of the frequency tuning. Then follows a treatment of optical pumping of the hyperfine levels in cesium, including results obtained in a cesium vapor cell with no buffer gas. Finally, we calculate the overpopulation between the ground state hyperfine levels and make comparisons with other proposed schemes for cesium maser operation.

2.0. PROPERTIES OF GaAs LASERS

In its simplest form a semiconductor diode laser consists of a p-n junction that is activated by injecting electrons into the conduction band[8]. The subsequent recombination of electrons and holes leads to the emission of radiation whose frequencies correspond approximately to the energy difference between the conduction and valence bands of the semiconductor material. The lasers are operated as diodes with steady-state or pulsed currents. Most cw lasers are run at liquid nitrogen temperature, although double-heterostructure lasers have been operated continuously at room temperature[9]. The power output from a single laser is of the order of watts, but this can be considerably increased in an array of many lasers[10]. The energy gap between the valence and conduction bands is controlled by

doping of the materials[11], by temperature[12], and even to a small extent by pressure[13], resulting in output wavelengths in the range from 6,300-9000 Å. When the current through the junction exceeds a certain threshold value, the emitted spectrum consists of a series of equally spaced, very sharp lines. On the other hand, for rates of injection below threshold, a several hundred Ångström wide recombination spectrum is emitted. Because of the small effective volume and aperture of the p-n junction, the radiation pattern is diffraction limited, with beam divergence of about 20° in a direction perpendicular to the junction plane. Furthermore, the radiation is strongly polarized with the electric field vector E perpendicular to the junction plane[14], although weaker modes with E parallel to the plane have also been observed[15].

Of particular importance in optical pumping experiments is the ability to adjust the laser frequency to the atomic transition frequency to be studied. The "coarse tuning" of the laser frequency can be accomplished by controlling the ambient temperature. Wittman[12], for instance, found that the wavelength of the laser light increased from 8400 to 8700 Å when the temperature was increased from 40 to 200°K. The additional "fine tuning" that is required to make the frequency of one of the laser modes coincide with or sweep through an atomic absorption line can be attained by controlling the current flowing through the diode junction, thereby controlling the temperature.

A comprehensive discussion of the "fine tuning" mechanism is the material for part 3 of this report.

The actual linewidth of a certain mode can only be measured with a Fabry-Perot interferometer[16] and gives a result of about 0.15MHz.

This is much less than the frequency separation of 9192 MHz between the cesium ground-state hyperfine levels. GaAs lasers have therefore been used to resolve the hyperfine splitting in a Cs by Siahatgar and Hochuli[17]. However, it was not within the framework of their investigation to study the implication of population inversion. In another experiment, Bölger and Diels[18] successfully used pulsed GaAs lasers to study the phenomenon of photon echoes in cesium vapor.

In the remaining part of this article we shall report on experimental results obtained with fast GaAs laser - pumping in a cesium vapor cell and discuss how this combination constitutes the basis for direct optically pumped cesium maser.

3.0. EXPERIMENTAL

A schematic diagram of the apparatus is shown in Fig. 8.

In this experiment a pulsed GaAs laser[19] emitting radiation around 8520 Å near room temperature was used to irradiate a cesium absorption cell with a vapor pressure of about 1×10^{-6} torr[20]. The cesium vapor serves as a fast, high resolution detector with properties such as transmission, re-emission, and speed of response determined by the atom temperature and number density. By means of this atomic type of detector one can observe the frequency sweep-rate of the laser with a higher accuracy and on a faster time scale than with conventional monochromators.

A schematic diagram of the ground state and first excited state of cesium is shown in Fig. 9. The $6^2S_{1/2}$ ground state consists of two hyperfine levels with F=4 and F=3, respectively, the levels being separated by 9162 MHz. The $6^2P_{3/2,\ 1/2}$ levels of cesium can be

FIGURE 8

SCHEMATIC OF APPARATUS USED FOR OPTICAL PUMPING OF CESIUM. The fluorescence radiation was detected with an RCA 7102 photomultiplier.

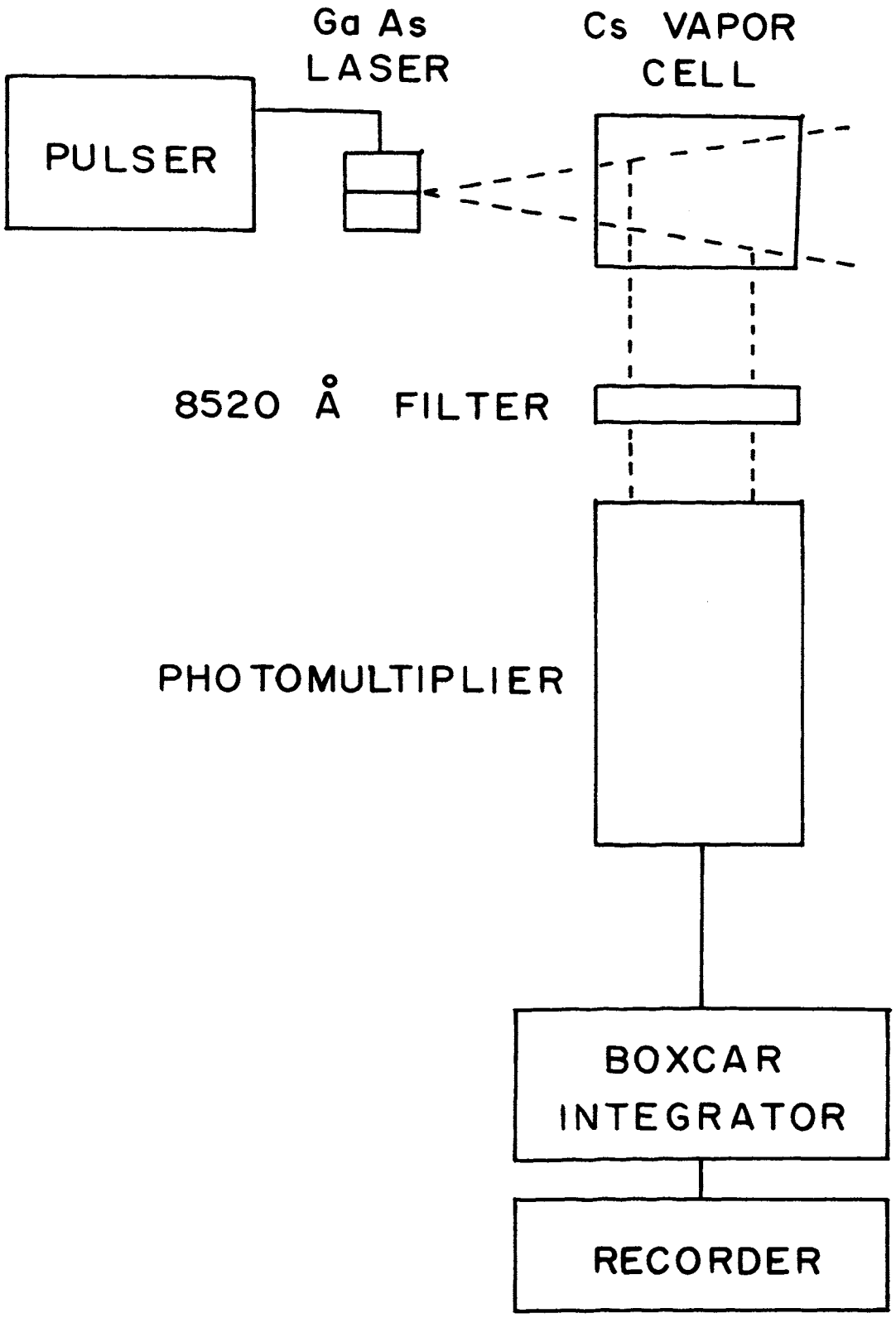
Ga As
LASER
Cs VAPOR
CELL
PULSER
8520 Å FILTER
PHOTOMULTIPLIER
BOXCAR
INTEGRATOR
RECORDER

Fig. 8

FIGURE 9

SIMPLIFIED TERM DIAGRAM FOR CESIUM. The notation is explained in the text following Eqs. (1-3).

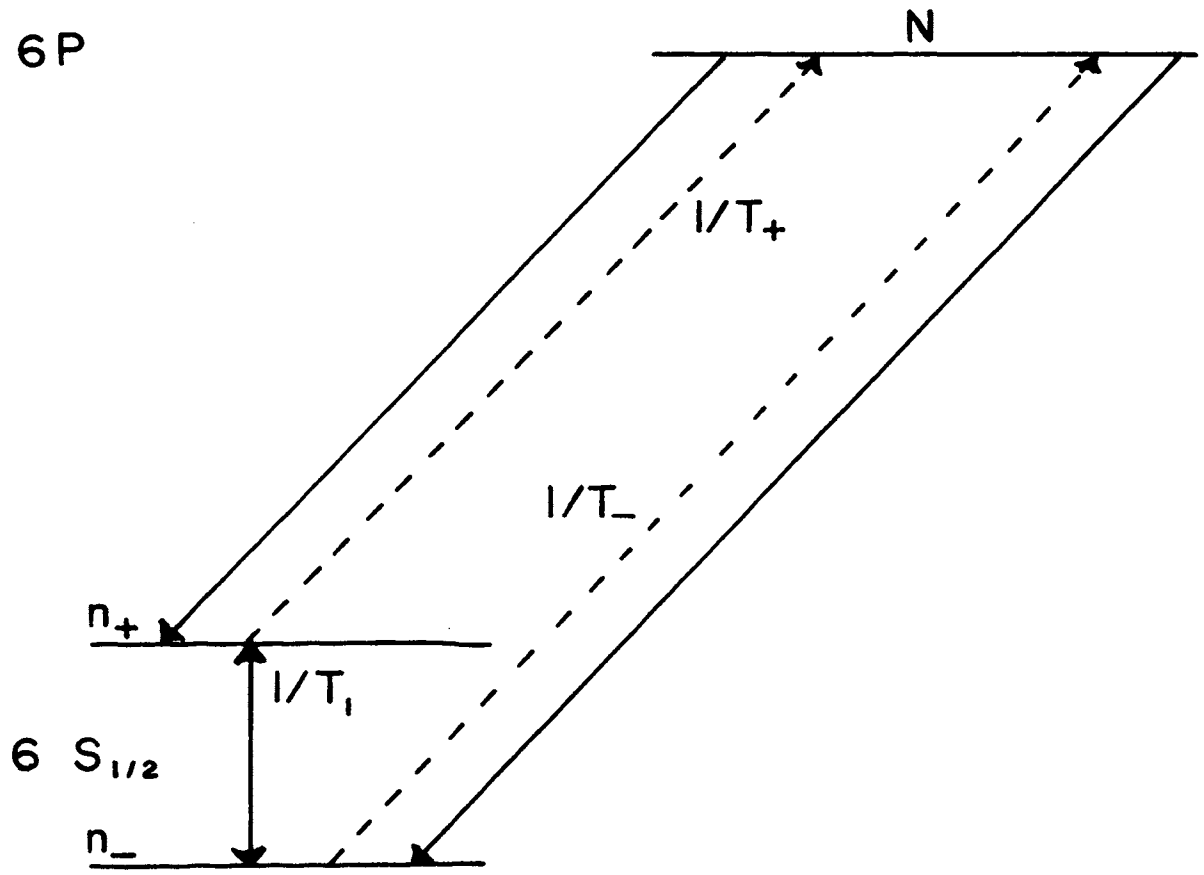

Fig. 9

excited by radiation of wavelength 8521 and 8944 Å, respectively, but only the first of these transition was utilized in the present work. For completeness, we have included in Fig.12 the F-values and sublevel spacings of the $6^2P_{3/2}$ state. However, because of Doppler broadening, the hyperfine structure of the excited state is not discernible in a vapor cell, and for this reason we shall in the following neglect the splitting and consider the $6^2P_{3/2}$ state discrete as indicated in the simplified Fig. 9. We note that in thermal equilibrium when no radiation is incident upon the atoms, the population densities of the ground state sublevels are nearly identical, since $\exp(-h\nu/kT)<<1$. (Here h is Planck's constant, ν = 9162 MHz, and T is the equilibrium temperature of the vapor cell.)

When radiation from a tunable laser impinges upon the atom system discussed above, absorption occurs at certain discrete frequencies. Characteristic of GaAs lasers is the heating of the junction during the current pulse which leads to a decrease in the frequency of the laser modes. Let us initially assume that the frequency ν_L of one particular laser mode is slightly larger than required for a $6^2S_{1/2}$ (F=3) → $6^2P_{3/2}$ transition, and then study the sequence of events as the laser frequency slowly decreases, as illustrated in Fig. 10. When the laser frequency $\nu_L = \nu_-$ (see Fig.10c) the $6^2P_{3/2}$ state is excited, and the subsequent re-emitted radiation is observed with the photomultiplier (Fig.10d). Laser radiation is not absorbed when $\nu_- > \nu_L > \nu_+$, and if the frequency sweep is sufficiently slow the photomultiplier is exposed to no light during the corresponding time interval. The next absorption and re-emission events occur when

FIGURE 10

PRINCIPLE OF FREQUENCY-SWEPT OPTICAL PUMPING EXPERIMENT.

a) Idealized step-function current pulse in laser.

b) Temperature rise in laser junction.

c) Illustration of frequency sweeping for a given laser mode. ν_- and ν_+ represent atomic transition frequencies from levels n_- and n_+ to the 6P-state.

d) Expected fluorescence signal as measured by the photomultiplier. (Arbitrary units on all axes.)

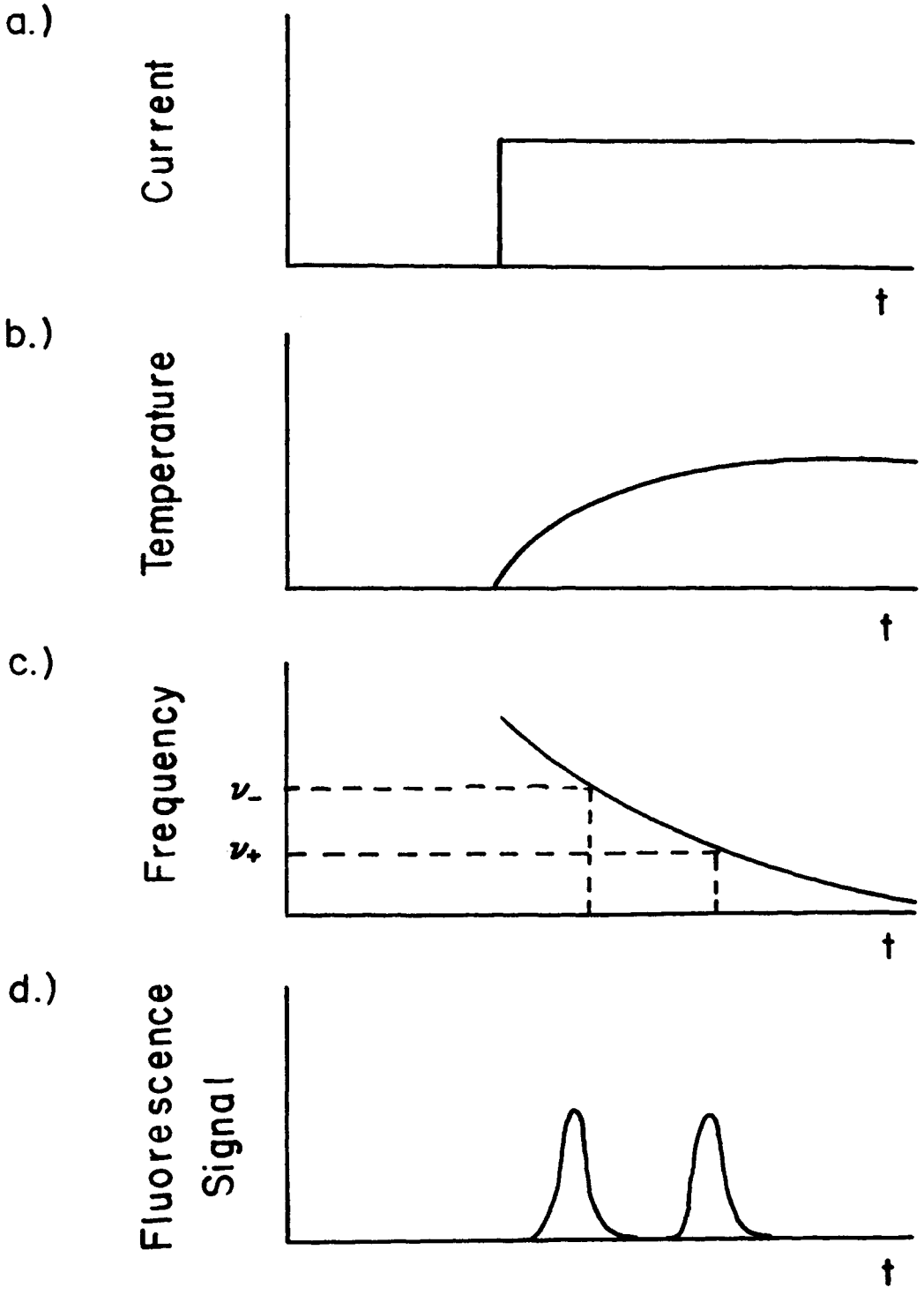
a.)
Current
t
b.)
Temperature
t
c.)
Frequency
ν_-
ν_+
t
d.)
Fluorescence
Signal
t

Fig. 10

$\nu_L = \nu_+$. The photomultiplier will, therefore, detect <u>two</u> pulses of flourescence light, one at the instant when $\nu_L = \nu_+$ and the other when $\nu_L = \nu_-$, as illustrated in Fig. 10d. It is important here to emphasize that the frequency resolution of the absorption process is very high because of the narrowness of the laser line, whereas the frequencies of re-emitted light from transitions ending on the two ground state sublevels cannot be separated by the broadband interference filter in front of the photomultiplier.

A typical observation made with the apparatus described in Fig. 8 is shown in Fig. 11. The result demonstrates all of the features in the previous discussion, and clearly reveals the predicted double-pulse of re-emitted radiation. In order to demonstrate that the double-signals were actually due to re-emission from the Cs vapor and not to other scattering and reflection effects, two consistency checks involving the absorption coefficient and the atomic lifetime were performed. The absorption coefficient was found from the spatial variation of the amplitude of the re-emitted pulse. An estimate of cesium number density[20] and use of Beer's law yielded a value for the absorption coefficient that agreed with the calculated number for similar experimental conditions to within a factor of 2. Furthermore, the falltime of the detected pulse was used as a measure of the lifetime of the excited state, giving a result of 36 ns. This is within 20 percent of previously published values[21]. The discrepancy can be accounted for by trapping of resonance radiation, as calculated from Holstein's theory[22], by the risetime of the detecting system, and by the temporal dependence of the laser light pulse.

FIGURE 11

RE-EMITTED LIGHT FROM THE CESIUM ABSORPTION CELL. The first pulse corresponds to the process $6^2S_{1/2}(F=3) + h\nu_- \rightarrow 6^2P_{3/2} \rightarrow 6^2S_{1/2}(F=3,F=4) + h\nu$ and the second pulse corresponds to the process $6^2S_{1/2}(F=4) + h\nu_+ \rightarrow 6^2P_{3/2} \rightarrow 6^2S_{1/2}(F=3,F=4) + h\nu$. The laser was driven by a current pulse with a peak amplitude of 25 A.

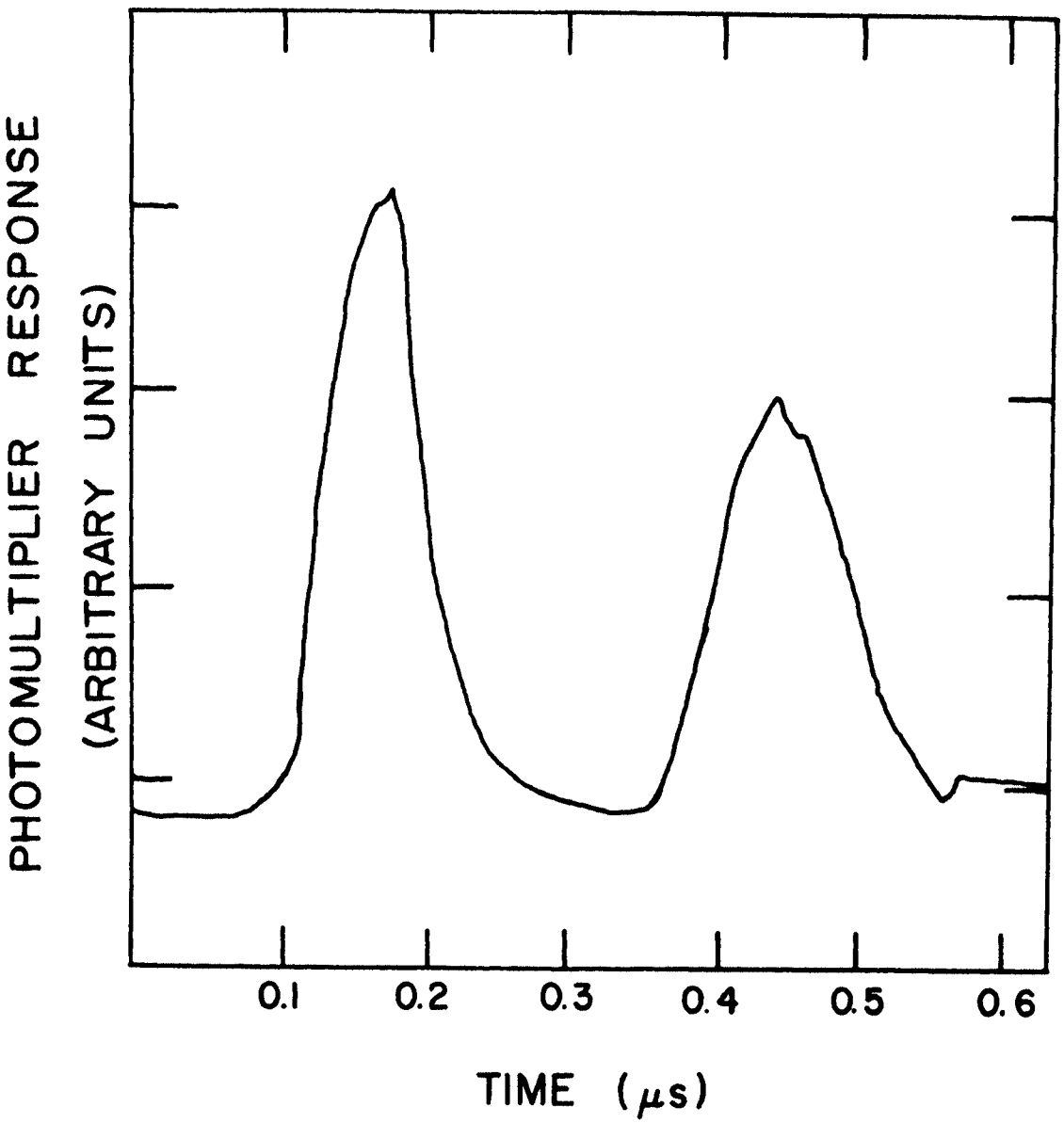
PHOTOMULTIPLIER RESPONSE
(ARBITRARY UNITS)
0.1
0.2
0.3
0.4
0.5
0.6
TIME (μs)

Fig. 11

By measuring the time interval between the two re-emitted pulses in Fig. 11, we determined the shift in wavelength with time to be 0.8 Å/ns. We note that this number represents an average over the actual sweeping time of 300 ns, and does not imply that the laser wavelength is a linear function in time.

An interesting feature illustrated in Fig. 11 is the disparity in amplitude between the two light pulses. Since the intensity of the re-emitted radiation is proportional to the intensity of the exciting radiation, the different amplitudes provide a measure of the temporal dependence of the laser intensity.

It is important to realize that the F=3 ground-state hyperfine level is being depopulated during the first fluorescence pulse in Fig. 11. An estimate of the corresponding population inversion and the feasibility of a GaAs laser-pumped Cs maser will be made in the following section.

4.0. RATE EQUATIONS

In the following discussion we shall consider the simplified term diagram shown in Fig. 9 but refer to the complete diagram in Fig. 12 for an evaluation of the number of Zeeman levels within each hyperfine state. Since we are only interested in transitions between the ground-state hyperfine levels, the structure of the excited state can be ignored, and we shall let N represent the total number of atoms in the 6P -state. Furthermore, for given values of m_F we shall define n_+ and n_- as the number of atoms in the upper and lower hyperfine levels, respectively. The total number of atoms in the system can then be expressed as

FIGURE 12

COMPLETE TERM DIAGRAM FOR CESIUM LEVELS RELEVANT TO MASER OPERATION. The separation between the energy levels is not to scale.

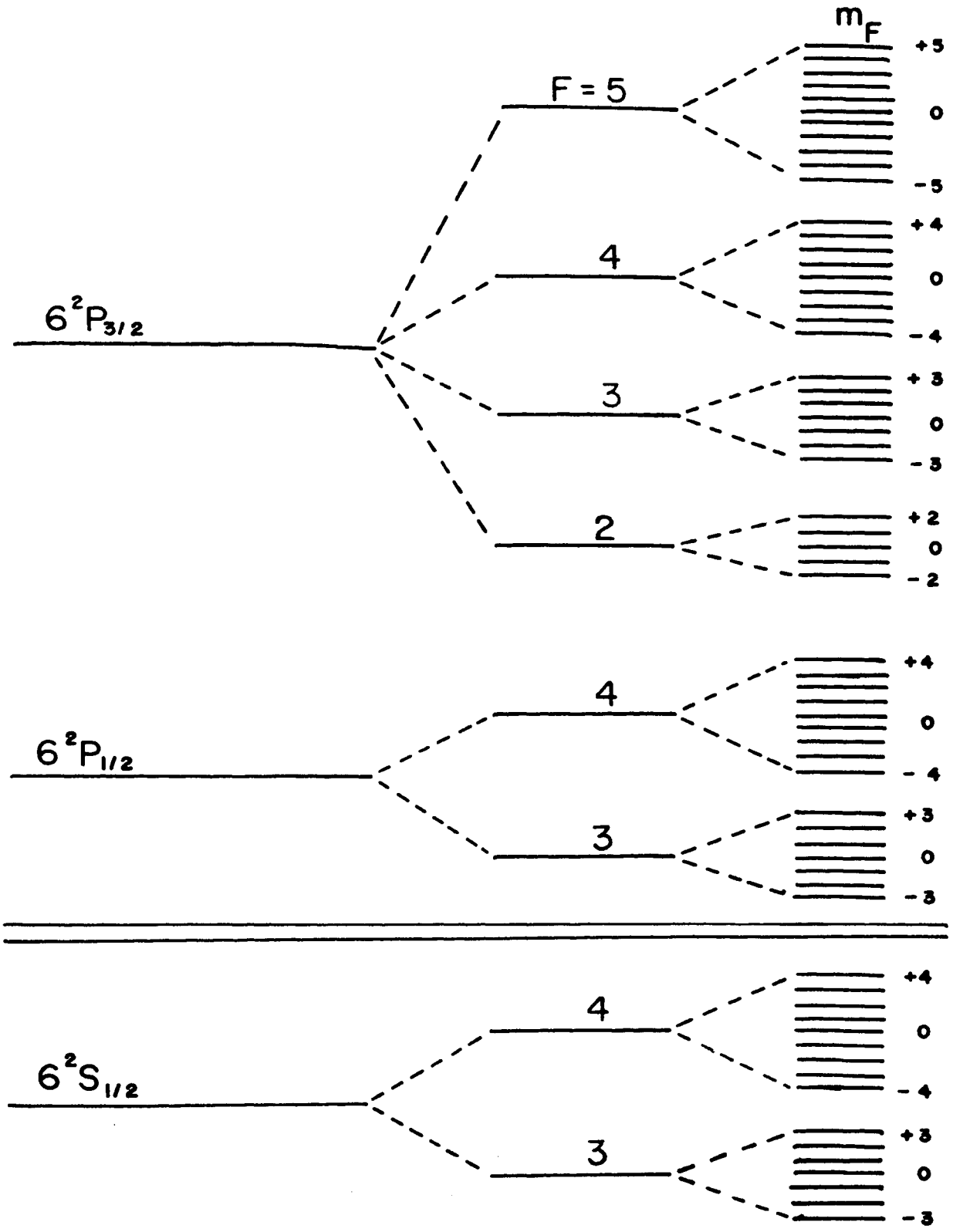
m_F
+5
0
-5
F = 5
+4
0
-4
4
$6^2P_{3/2}$
+3
0
-3
3
+2
0
-2
2
+4
0
-4
4
$6^2P_{1/2}$
+3
0
-3
3
+4
0
-4
4
$6^2S_{1/2}$
+3
0
-3
3

Fig. 12

$$n = N + (2I + 2)\, n_+ + 2I n_- \,, \tag{4}$$

where $I = 7/2$ for cesium. With the interactions included in Fig. 9 we can write the rate equations[23] for the hyperfine levels as follows:

$$dn_+/dt = -(n_+/T_+) - (n_+ - n_{eq})/T_1 + N/[2(2I+1)\tau] \tag{5}$$

$$dn_-/dt = -(n_-/T_-) - (n_- - n_{eq})/T_1 + N/[2(2I+1)\tau] \tag{6}$$

Since $n_{eq} = (n-N)/[2(2I+1)]$ is the number of atoms in a given ground-state Zeeman level in thermal equilibrium, the terms $(n_+ - n_{eq})$ and $(n_- - n_{eq})$ in Eqs. (5) and (6) describe deviations from equilibrium. The 6P -state will decay into the 6S -state with a lifetime τ, and will be populated from the n_+ and n_- levels by the rates $1/T_+$ and $1/T_-$, respectively. The relaxation between Zeeman levels is accounted for by the time T_1. From Eqs. (4-6) one can solve for the overpopulation $(n_+ - n_-)$, without the need for an additional rate equation for the 6P -state. The result is

$$\frac{n_+ - n_-}{n} = \frac{(1/T_-) - (1/T_+)}{\frac{2(2I+1)}{T_1} + \frac{2(I+1)}{T_-} + \frac{2I}{T_+}} \,, \tag{7}$$

which is obtained by assuming N much smaller than the other terms in Eq. (4).

The limitation of the model depicted in Fig. 9 is that induced transition between the hyperfine levels are not included[24]. Even so, the result is capable of predicting small overpopulations, and has been used for previous calculations in rubidium and cesium[25].

5.0. GaAs LASER-PUMPING

The following features are of importance when using GaAs lasers for pumping of cesium vapor masers: First, we note that a preselected Fabry-Perot mode can be accurately tuned to coincide with the lower F=3 hyperfine level, thus providing a source of highly filtered radiation, i.e., $(1/T_-)>>(1/T_+)$. Since the other laser modes are several Ångströms apart from the mode that is used to depopulate the n_- -level, there is no need for additional filtering as in the rubidium maser. Furthermore, the spectral power output in the pumping mode is of the order of one watt or more. In other words, the radiation is intense, i.e., $(1/T_-)>>(1/T_1)$. Within the constraints of this theory, the relative overpopulation will approach a maximum value of 1/9, as shown in Fig. 13 where the ratio between the pumping and relaxation rates is equal to T_1/T_-.

It is of interest to compare the maximum overpopulation attainable with GaAs laser with the work of Franz[2]. By pumping cesium with (σ^+) D_1 $(^2S_{1/2} \rightarrow {}^2P_{1/2})$ radiation in the presence of a heavy noble gas, he obtained a maximum relative overpopulation of 0.015. Note that a GaAs laser operating around 8944 Å can be used to pump the $6^2P_{1/2}$ -state, thereby taking advantage of the smaller collisional relaxation rate from this state as compared to the J = 3/2 state[25].

FIGURE 13

THE RELATIVE OVERPOPULATION $(n_+-n_-)/n=(T_1/T_-)/[16+9(T_1/T_-)]$ AS A FUNCTION OF T_1/T_-. The parameter T_1/T_- is a measure of the pumping rate over the relaxation rate.

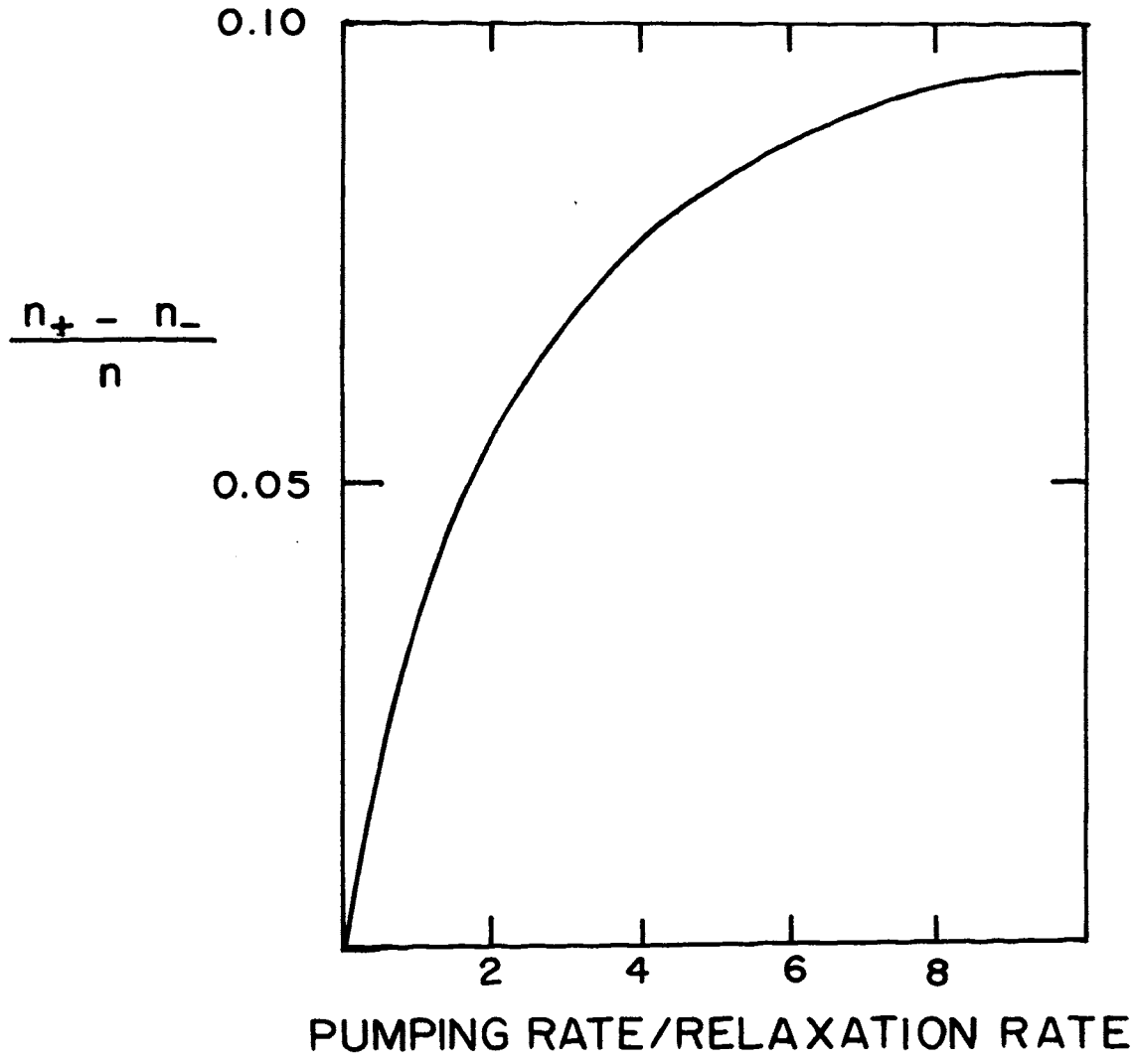

Fig. 13

REFERENCES

* Supported in part by the Office of Naval Research and the National Science Foundation.

1. N.F. Ramsey, Molecular Beams, (Oxford at the Clarendon Press, 1956), pp. 283-285.
See also A.O. Coubrey, Proc. IEEE 54, 116 (1966).

2. F.A. Franz, Appl. Phys. Letters 16, 391 (1970).

3. E.C. Beaty, P.L. Bender, and A.R. Chi, Phys. Rev. 112, 450 (1958).

4. To the authors' knowledge, experimental results confirming this idea have not been published.

5. In conjunction with this effort the same type of laser has been used in another experiment to study photoionization of excited cesium atoms. Preliminary results have been discussed by R.E. Hebner, Jr., and K.J. Nygaard, IEEE Conference Redord of 1970 Thermionic Conversion Specialist Conference, October 26-29, 1970, pp. 323-326.

6. P. Davidovits and R. Novick, Proc. IEEE 54, 155 (1966).

7. The Rb^{85} maser has been discussed by J. Vanier, R. Vaillancourt, G. Missout, and M. Tetu, J. Appl. Phys. 41, 3188 (1970).

8. An excellent review is found in C.H. Gooch, Gallium Arsenide Lasers, (Wiley-Interscience, 1969).

9. I. Hayashi, M.B. Panish, P.W. Foy, and S. Sumski, Appl. Phys. Letters 17, 109 (1970).

10. W.E. Ahearn and J.W. Crowe, IEEE J. Quantum Electronics, QE-6, 377 (June 1970). This issue is specially devoted to semiconductor lasers and contains a total of 30 articles.

11. H. Kressel, H.F. Lockwood, and H. Nelson, loc. cit. 6, 278 (1970). The lower wavelength region is obtained with $Al_xGa_{1-x}As$ - lasers.

12. F.W. Lindner, Physics Letters 24A, 409 (1967).
H.R. Wittman, Rev. Sci. Instr. 39, 1382 (1968).

13. G. Fenner, J. Appl. Phys. 34, 2955 (1963).

14. N.E. Byer and J.K. Butler, IEEE J. Quantum Electronics QE-6, 291 (1970).

15. V.N. Alyamovskii, V.S. Bagaev, Yu.N. Berozashvili, and B.M. Vul, Fizika Tverdogo Tela 8, 1091 (1966). (Soviet Physics - Solid State 8, 871 (1966).)

16. W.E. Ahearn and J.W. Crowe, IEEE J. Quant. Elec. QE-2, 196 (1965).

17. S. Siahatgar and U.E. Hochuli, IEEE J. Quant. Elec. QE-5, 295 (1969).

18. B. Bölger and J.C. Diels, Physics Letters 28A, 401 (1968).

19. Model ML1 fabricated by the Monsanto Corporation.

20. Vapor pressure data for cesium are found in R.E. Honig, RCA Rev. 23, 567 (1962); J.B. Taylor and I. Langmuir, Phys. Rev. 51, 753 (1937); R. Hultgren, R.L. Orr, P.D. Anderson, and K.K. Kelly, Selected Values for the Thermodynamic Properties of Metals and Alloys (John Wiley and Sons, Inc., New York, 1963), p. 87; A.N. Nesmeyanov, Vapor Pressure of the Chemical Elements, R. Gary, Ed. (Elsevier Publ. Co., Amsterdam, 1963), pp. 146-150; M. Rozwadowski and E. Lipworth, J. Chem. Phys. 43, 2347 (1965); L.L. Marino, A.C.H. Smith, and E. Caplinger, Phys. Rev. 128, 2243 (1962); and U. Buck and H. Pauly, Z. Physik. Chemie Neue Folge 44, 345 (1965).

21. J.K. Link, J. Opt. Soc. Am. 56, 1195 (1966).

22. T. Holstein, Phys. Rev. 83, 1159 (1951).

23. F. Hartmann, Journal de Physique 28, 288 (1967). The same set of equations has been used by Franz (Ref. 2) and by Vanier et al. (Ref. 7) for studies of rubidium and cesium.

24. A more complete theory including the effects of the pumping light and induced transitions has been formulated by J. Vanier, Phys. Rev. 168, 129 (1968).

25. J. Fricke, J. Haas, E. Luscher, and F.A. Franz, Phys. Rev. 163, 45 (1967).

APPENDIX II

MODAL BEHAVIOR AND TEMPERATURE TUNING OF PULSED ROOM-TEMPERATURE GaAs LASERS

This material has been accepted for publication in Physica and is currently in press.

Modal Behavior and Temperature Tuning of Pulsed Room-Temperature GaAs Lasers

The wavelength shift of a single mode of a pulsed, room-temperature GaAs laser was studied using the energy separation of the two hyperfine levels of the $6^2S_{1/2}$-state of cesium to define a fixed wavelength interval. A lineshift coefficient of 10^{-3} Å A^{-2} μsec^{-1} for a single mode was measured. This coefficient is approximately two orders of magnitude smaller than the lineshift coefficient for the envelope of a family of modes. The predominant physical mechanism for the wavelength shift of a single mode appears to be the change in the index of refraction of the laser cavity with a change in junction temperature during a pulse.

1.0. INTRODUCTION

Due to their thermal tunability, high brightness, commercial availability, and ease of use, gallium arsenide (GaAs) lasers lend themselves as attractive sources for excitation of atomic and molecular systems[1]. We are presently using GaAs lasers to study photoionization of excited cesium atoms[2] and to induce maser transitions[3] in cesium vapor. The objective of this paper is to report results pertaining to the modal behavior and tuning mechanisms for the lasers used in these investigations. In steady-state, the mode behavior has been adequately explained[4], whereas the tuning mechanism for pulsed operation is not completely understood.

In this section we first describe the principles and characteristics of semiconductor lasers, with special emphasis on GaAs lasers. The experimental section includes the laser emission spectrum which exhibits the typical Fabry-Perot modes. The frequency-temperature dependence of a given mode is then studied by scanning the laser frequency over the cesium ground-state hyperfine levels, using the difference between the $6\,^2S_{1/2}$, F=4 and F=3 levels as a calibrated frequency interval. On the basis of the experimental results we conclude that the predominant frequency tuning mechanism arises from the temperature dependence of the refractive index of the laser medium.

2.0. CHARACTERISTICS OF GaAs LASERS

In its simplest form a semiconductor diode laser consists of a p-n junction that is activated by injecting electrons into the conduction band[5]. The subsequent recombination of electrons and holes leads to the emission of radiation whose frequencies correspond approximately to the energy difference between the conduction and valence bands of the semiconductor material. The lasers are operated as diodes with constant or pulsed currents. Most cw lasers are run at liquid nitrogen temperature, although double-heterostructure lasers have been operated continuously at room temperature[6]. The power output from a single laser is of the order of watts, but this can be considerably increased in an array of many lasers[7]. The energy gap between the valence and conduction bands is controlled by doping of the material[8],

by temperature[9], and even to a small extent by pressure[10], resulting in output wavelengths in the range from 6,300-9000 Å. When the current through the junction exceeds a certain threshold value, the emitted spectrum consists of a series of equally spaced, very sharp lines. On the other hand, for rates of injection below the threshold current a several hundred Ångström wide recombination spectrum is emitted. Because of the small effective volume and aperture of the p-n junction, the radiation pattern is diffraction limited, with beam divergence of about 20° in a direction perpendicular to the junction plane. Furthermore, the radiation is strongly polarized with the electric field vector $\vec{E}$ perpendicular to the junction plane[11], although weaker modes with $\vec{E}$ parallel to the plane have also been observed[12].

Of particular importance in optical pumping experiments is the ability to adjust the laser frequency to the atomic transition frequency to be studied. The "coarse tuning" of the laser frequency can be accomplished by controlling the ambient temperature. Wittman[9], for instance, found that the wavelength of the laser light increased from 8400 to 8700 Å when the temperature was increased from 40 to 200°K. The additional "fine tuning" that is required to make the frequency of one of the laser modes coincide with or sweep through an atomic absorption line can be attained by controlling the current flowing through the diode junction.

3.0. EXPERIMENTAL PROCEDURE AND RESULTS

The lasers[13] we have studied have been operated in the pulsed mode with a pulse generator capable of supplying a maximum of 30 amps for a pulse width at half maximum of about 200 nsec. With a repetition rate of 100 pps, the spectrum shown in Fig. 14 was obtained using a Jarrell-Ash 1/2 meter spectrometer. The photomultiplier signal was analyzed by a boxcar integrator[14], and pertains to a time 75 nsec after the current pulse was applied. At other times during the current pulse, the wavelength of a certain mode will change very slightly due to ohmic heating, but the change would not be discernible on the wavelength scale used in Fig.14. Also, at later times during the current pulse more and more long-wavelength laser modes are excited as the shorter-wavelength modes disappear[15].

The temperature dependence of a certain mode can be studied by observing the change in wavelength $\Delta\lambda$ that takes place during a time interval Δt. Since the actual changes during a short pulse are less than 0.5 Å, small optical monochromators do not exhibit sufficient resolution for this measurement. As an alternative, we have chosen to work with a fixed wavelength interval of $\Delta\lambda$ = 0.22 Å, corresponding to the hyperfine splitting of the $Cs6^2S_{1/2}$ groundstate. (Transitions between the F=3 and F=4 hyperfine levels correspond to a frequency of 9162 MHz.) For a laser frequency increasing in time the lower hyperfine $6^2S_{1/2}$ (F=3) level will absorb radiation slightly before the (F=4) -level. The subsequent re-emission from the $6^2P_{3/2}$ state[16] will occur in two pulses, with time separation equal to the time between the two absorption events. This effect has been observed by Siahatgar

FIGURE 14

SPECTRUM OF THE RADIATION EMITTED FROM THE GaAs LASER. The observation was made 75 ns after the beginning of the current pulse.

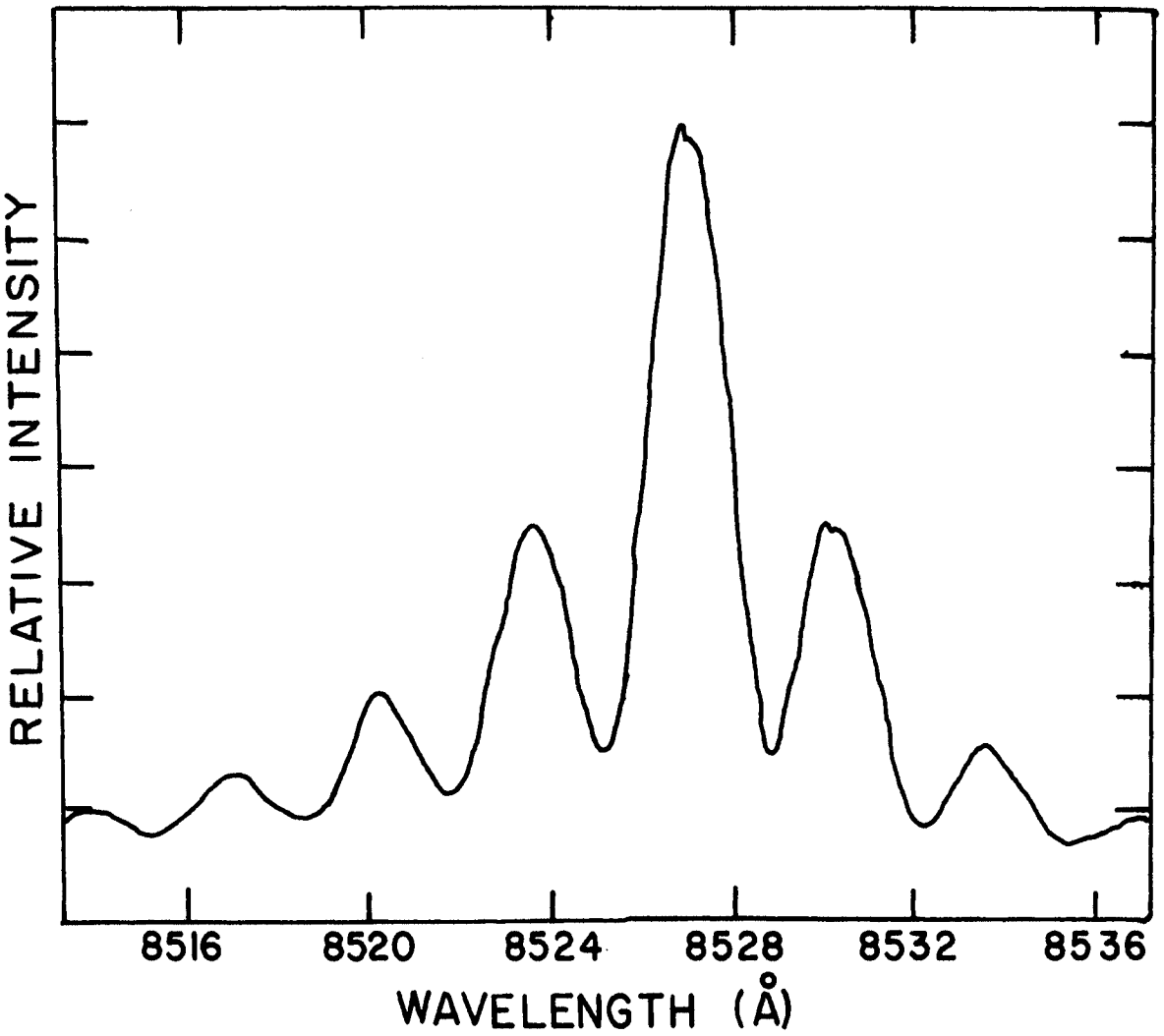
RELATIVE INTENSITY
8516
8520
8524
8528
8532
8536
WAVELENGTH (Å)

Fig. 14

and Hochuli[17] for GaAs lasers operating at liquid nitrogen temperature, and in our laboratory for pulsed lasers near room temperature[18]. According to our experience, the double-pulse of re-emitted fluorescence radiation constitutes a simple method for defining an accurate wavelength interval on a fast time scale. Along these lines, we want to indicate the applicability of frequency-swept GaAs lasers in fast, high-resolution spectroscopic experiments.

The experimental arrangement is so simple that a special illustration is not warranted. The radiation from a pulsed GaAs laser impinges upon an absorption cell filled with cesium vapor to a pressure of about 10^{-6} torr[19]. The re-emitted resonance radiation is observed at a direction perpendicular to the incident axis by means of a photomultiplier[20]. A narrow-band (150 Å) interference filter is put in front of the photomultiplier to reduce the intensity of background radiation. It is important here to emphasize that the spectral resolution of the absorption process is very high because of the narrowness of the laser line, whereas, the frequencies of the re-emitted light from transitions ending on the two ground-state sublevels are not resolved with the filter-detector system used in the experiment. The photomultiplier output is monitored by an oscilloscope, and the time interval Δt between the two re-emitted light pulses sufficies to calculate $\Delta\lambda/\Delta t$ for the laser at a wavelength of 8521 Å. Typically, for a selected laser mode, we found $\Delta\lambda/\Delta t = 0.8$ Å/μsec. The same result applies to all permitted modes within the laser cavity. We note that this number represents an average over the actual time interval and does not imply that the laser wavelength is a linear function in time.

4.0. DISCUSSION

To compare the results reported here with those of other workers, it is advantageous to introduce a line shift coefficient, ξ, as defined by Gonda *et al.*[15] by the expression

$$\Delta\lambda(t) = \xi I^2 t \quad .$$

In their model the shift in wavelength, $\Delta\lambda$, is caused by a square-wave current pulse of amplitude I(A) and duration t(μsec). The coefficient ξ has been found to be independent of current if ohmic heating is the predominent power dissipation mechanism in the laser. The pertinent parameters of their experiment are summarized in Table I.

TABLE I. Comparison of Experimental Parameters and Wavelength Shift Coefficients

Reference	Spectral Resolution (Å)	Operating Temperature (°K)	I(A)	Pulse Duration (μsec)	ξ (Å A^{-2} μsec^{-1})
Gonda *et al.*[a]	1-6.5	7	3-6	10	3.2×10^{-1}
Gooch[b]	1-2	77	10	20	4×10^{-3}
Present	0.2	300	25	0.3	1.2×10^{-3}

[a]reference 15

[b]reference 21

Also included in Table I are the results of Gooch[21] who measured the temporal dependence of the output of a laser operating near 77°K during 10A, 20 μsec current pulse. With a wavelength resolution of

1 - 2Å, he was able to separate the individual modes of a family. From his data, a line shift coefficient for an individual mode of 4×10^{-3} Å A^{-2} μsec^{-1} was calculated. In spite of the significant differences in operating temperature and pulse duration, the results of Gooch agree closely with the present data. However, our value for ξ is a factor of 100 less than that obtained by Gonda et al. The objective of the following discussion is to resolve this discrepancy.

It is important to realize that the disagreement between the latter two values and that obtained by Gonda et al. is directly related to the resolution of the apparatus. A low-resolution apparatus will measure the shift of the envelope of a family of modes, while a high-resolution apparatus detects the shift of an individual mode.

The mechanisms for the individual mode wavelength shift can be studied from the relation

$$m\lambda_m = 2nL \quad , \tag{1}$$

where m is an integer, λ_m is the wavelength of a given Fabry-Perot mode, n is the index of refraction of the cavity, and L is the length of the cavity. The physical effects associated with heating of the laser are thermal expansion of the cavity length and changes in the index of refraction. (Note that the index is a function of both temperature and wavelength.) Taking the derivative of Eq. (1) with respect to temperature and rearranging terms, we obtain

$$[1/\lambda_m - (1/n)(\partial n/\partial\lambda)_T]d\lambda_m/dT = (1/L)(dL/dT) + (1/n)(\partial n/\partial T)_\lambda . \tag{2}$$

From published data on the coefficient of linear expansion[22] for GaAs, we find L^{-1} $(dL/dT) \approx 7 \times 10^{-6}$ $(°K)^{-1}$, which is one order of

magnitude less the last term[23] on the right-hand side of Eq. 2. An upper bond for the term $n^{-1}\ (\partial n/\partial\lambda)_T$ would be 5×10^{-5} Å^{-1}, which is less, but not much less than λ_m^{-1}. With this restriction in mind, we can write

$$(1/\lambda_m)(d\lambda m/dT) \simeq (1/n)(dn/dT) \qquad (3)$$

The order-of-magnitude argument used here is not conclusive, but tends to support the hypothesis that the temperature tuning of a single mode can be ascribed to the temperature dependence of the refractive index. Furthermore, the model represents a simplification as compared to an actual diode junction, since the spatial dependence of the refractive index[4] and thermal dissipation are not included. Even so, our model is useful for predicting approximately the wavelength shift of a single mode due to ohmic heating.

An expression for the wavelength scan-rate is obtained by multiplying Eq. (3) by dT/dt:

$$(1/\lambda_m)(d\lambda_m/dt) - (1/n)(dn/dT)(dT/dt) \qquad (4)$$

An estimate for dT/dt is obtained from the first order theory of Gooch[21], which, when combined with the other numbers discussed above gives $d\lambda_m/dt \approx 2.7$ Å μsec^{-1} The calculated value is thus within a factor of four of our measured value of 0.8 Å μsec^{-1} This comparison, therefore, lends confidence to our hypothesis that the frequency shift is predominately caused by the temperature dependence of the GaAs index of refraction.

CONCLUSIONS

In pulsed GaAs lasers both the frequency and intensity of an individual cavity mode change due to ohmic heating of the junction. The wavelength shift of an individual mode is described by the coefficient $\xi \simeq 10^{-3}$ Å A^{-2} μsec^{-1}, whereas the corresponding coefficient for the spectral envelope is a factor of 100 larger. We have found that the single-mode tuning mechanism is due predominately to the temperature dependence of the index of refraction of the laser material, while the overall shift in the wavelength of the recombination radiation stems from the temperature dependence of the energy gap. The salient feature of the experiment was to utilize the hyperfine structure of the cesium ground-state atom to define both a fixed frequency and frequency interval. Whereas previous experiments were conducted at low temperature with long current pulses, we operated the GaAs laser at room temperature with short pulses and obtained results in essential agreement with those of Gooch[21].

REFERENCES

1. A similar type of device, the $Pb_{1-x}Sn_xTe$ laser has recently been used to detect pollutants in the atmosphere. See E.D. Hinkley and P.L. Kelley, Science 171, 635 (1971).

2. R.E. Hebner, Jr. and K.J. Nygaard, IEEE Conference Record of 1970 Thermionic Conversion Specialist Conference, Miami Beach, Florida, October 26-29, 1970, pp. 323-326.

3. K.J. Nygaard and R.E. Hebner, Jr., to be published.

4. T.L. Paoli, J.E. Ripper, and T.H. Zachos, IEEE J. Quant. Electronics QE-5, 271 (1969).

5. An excellent review is found in C.H. Gooch, Gallium Arsenide Lasers, (Wiley-Interscience, 1969).

6. I. Hayashi, M.B. Panish, P.W. Foy, and S. Sumski, Appl. Phys, Letters 17, 109 (1970).

7. W.E. Ahearn and J.W. Crowe, IEEE J. Quantum Electronics QE-6, 377 (June 1970). This issue is specially devoted to semiconductor lasers and contains a total of 30 articles.

8. H. Kressel, H.F. Lockwood, and H. Nelson, loc. cit. 6, 278 (1970). The lower wavelength region is obtained with $Al_xGa_{1-x}As$ - lasers.

9. F.W. Lindner, Physics Letters 24A, 409 (1967); H.R. Wittman, Rev. Sci. Instr. 39, 1382 (1968).

10. G. Fenner, J. Appl. Phys. 34, 2955 (1963).

11. N.E. Byer and J.K. Butler, IEEE J. Quantum Electronics QE-6, 291 (1970).

12. V.N. Alyamovskii, V.S. Bagaev, Yu.N. Berozashvili, and B.M. Vul, Fizika Tverdogo Tela 8, 1091 (1966). (Soviet Physics - Solid State 8, 871 (1966).)

13. Model ML 1 fabricated by Monsanto Corporation. The results obtained with these lasers are also applicable to devices made by other manufacturers.

14. Princeton Applied Research Model 160.

15. T. Gonda, H. Junker, and M.F. Lamorte, IEEE J. Quantum Electronics QE-1, 159 (1965).

16. Because of Doppler broadening the hyperfine structure of the $6^2P_{3/2}$-state is not resolved in a vapor cell.

17. S. Siahatgar and U.E. Hochuli, IEEE J. Quantum Electronics QE-5, 295 (1969).

18. See reference 3.

19. Vapor pressure data for cesium are found in R.E. Honig, RCA Rev. 23, 567 (1962); J.B. Taylor and I. Langmuir, Phys. Rev. 51, 753 (1937); R. Hultgren, R.L. Orr, P.D. Anderson, and K.K. Kelly, Selected Values for the Thermodynamic Properties of Metals and Alloys (John Wiley and Sons, Inc., New York, 1963), p. 87; A.N. Nesmeyanov, Vapor Pressure of the Chemical Elements, R. Gary, Ed. (Elsevier Publ. Co., Amsterdam, 1963), pp. 146-150; M. Rozwadowski and E. Lipworth, J. Chem. Phys. 43, 2347 (1965); L.L. Marino, A.C.H. Smith, and E. Caplinger, Phys. Rev. 128, 2243 (1962); and U. Buck and H. Pauly, Z. Physik. Chemie Neue Folge 44, 345 (1965).

20. RCA 7102 refrigerated by a flow of cold nitrogen.

21. C.H. Gooch, Phys. Letters 16, 5 (1965).

22. E.D. Pierron, D.L. Parker, and J.B. McNeeley, Acta Cryst. 21, 290 (1966).

23. D.T.F. Marple, J. Appl. Phys. 35, 1241 (1964).